

Gaussian and Student's t mixture vector autoregressive model with application to the asymmetric effects of monetary policy shocks in the Euro area

Savi Virolainen
University of Helsinki

Abstract

A new mixture vector autoregressive model based on Gaussian and Student's t distributions is introduced. As its mixture components, our model incorporates conditionally homoskedastic linear Gaussian vector autoregressions and conditionally heteroskedastic linear Student's t vector autoregressions. For a p th order model, the mixing weights depend on the full distribution of the preceding p observations, which leads to attractive theoretical properties such as ergodicity and full knowledge of the stationary distribution of $p + 1$ consecutive observations. A structural version of the model with statistically identified shocks and a time-varying impact matrix is also proposed. The empirical application studies asymmetries in the effects of the Euro area monetary policy shock. Our model identifies two regimes: a high-growth regime that is characterized by positive output gap and mainly prevailing before the Financial crisis, and a low-growth regime that characterized by negative but volatile output gap and mainly prevailing after the Financial crisis. The average inflationary effects of the monetary policy shock are stronger in the high-growth regime than in the low-growth regime. On average, the effects of an expansionary shock are less enduring than of a contractionary shock. The CRAN distributed R package `gmvarKit` accompanies the paper.

Keywords: mixture vector autoregression, regime-switching, Student's t mixture, Gaussian mixture, mixture model, Euro area monetary policy shock

The author thanks Markku Lanne, Mika Meitz, and Pentti Saikkonen for discussions and comments, which helped to improve this paper substantially. The author also thanks Leena Kalliovirta for the useful comments and Academy of Finland for the financial support (Grant 308628).

Contact address: Savi Virolainen, Faculty of Social Sciences, University of Helsinki, P. O. Box 17, FI-00014 University of Helsinki, Finland; e-mail: savi.virolainen@helsinki.fi.

The author has no conflict of interest to declare.

1 Introduction

Mixture autoregressive models are useful for modelling series in which the data generating dynamics vary in time. Such variation may arise due to wars, crises, business cycle fluctuations, or policy shifts, for example. Mixture autoregressive models can be described as collections of (typically linear) autoregressive models, which are called mixture components, components processes, or regimes. At each time point, the process generates an observation from one of its mixture components that is randomly selected according to the probabilities given by the mixing weights.

Several new mixture autoregressive models have been introduced recently. Kalliovirta, Meitz, and Saikkonen (2015) introduced the Gaussian mixture autoregressive (GMAR) model, which incorporates linear Gaussian autoregressions as its mixture components and mixing weights that, for a p th order model, depend on the full distribution of the previous p observations. The specific definition of the mixing weights leads to attractive theoretical and practical properties, such as ergodicity and full knowledge of the stationary distribution of $p + 1$ consecutive observations. Kalliovirta, Meitz, and Saikkonen (2016) introduced a multivariate version of this model, the Gaussian mixture vector autoregressive (GMVAR) model, which employs linear Gaussian vector autoregressions (VAR) as its mixture components and has analogous properties to the GMAR model. Burgard, Neuenkirch, and Nöckel (2019), in turn, proposed a model with linear Gaussian VARs as mixture components, and mixing weights that depend on switching variables through a logistic function. Meitz, Preve, and Saikkonen (forthcoming) introduced the Student's t mixture autoregressive (StMAR) model with analogous properties to the GMAR model, but incorporating conditionally heteroskedastic mixture components based on Student's t -distribution. Virolainen (forthcoming) introduced the Gaussian and Student's t mixture autoregressive (G-StMAR) model, where some of the mixture components are based on a Gaussian distribution and some on a t -distribution.

This paper introduces a multivariate version of the G-StMAR model, and as a special case also a multivariate version of the StMAR model. The Gaussian and Student's t mixture vector autoregressive (G-StMVAR) model accommodates conditionally homoskedastic linear Gaussian VARs and conditionally heteroskedastic linear Student's t VARs as its mixture components. Both types of mixture components have the same form for the conditional mean, a linear function of the preceding p observations, but the conditional covariance matrices are different. The linear Gaussian VARs have constant conditional covariance matrices. The conditional covariance matrices of the linear Student's t VARs, in turn, consist of a constant covariance matrix multiplied by a time-varying scalar that depends on the quadratic form of the previous p observations. In this sense, the conditional covariance is of ARCH (autoregressive conditional heteroskedasticity) type. But since it is just a time-varying scalar multiplying the constant covariance matrix, it is not as general as the conventional multivariate ARCH process that allows the entries of the conditional covariance matrix to vary relative to each other (e.g., Lütkepohl, 2005, Section 16.3). The specific formulation of the conditional covariance matrix is, nonetheless, convenient for establishing stationary properties similar to the linear Gaussian VARs. Our specification of the conditional covariance matrix is also parsimonious, as it only depends on the degrees of freedom and the autoregressive parameters (in addition to the parameters in the constant covariance matrix). This is particularly advantageous in the context of mixture VARs, as the large number of parameters may often be a problem even without an ARCH component.

For a p th order G-StMVAR model, the mixing weights are defined as weighted ratios of the components process stationary densities corresponding the previous p observations. This formulation is appealing, as it states that the greater the relative weighted likelihood of a regime is, the more likely the process is to generate an observation from it. This is a convenient feature for forecasting, and it also facilitates associating statistical characteristics and economic interpretations to the regimes. It turns out that the specific formulation of the mixing weights also leads to attractive theoretical properties, such as ergodicity and full knowledge of the stationary distribution of $p + 1$ consecutive observations. In contrast to the GMVAR model, our model is able to capture excess kurtosis and conditional heteroskedasticity within the regimes. If all of the regimes are assumed to be linear Student's t VARs, a multivariate version of the StMAR model is obtained as a special case. We refer to this model as the StMVAR model.

In addition to the reduced form model, we propose a structural version of the G-StMVAR model that generalizes the SGMVAR model of Virolainen (2022) to accommodate conditionally heteroskedastic Student's t regimes. The SG-StMVAR model incorporates a time-varying impact matrix that varies according to the conditional variance of the reduced form error. As a consequence of a single (time-varying) impact matrix, identification of the shocks requires that the error term covariance matrices are simultaneously diagonalized in all regimes. Together with a constant normalization of the structural error's conditional covariance matrix, this condition generally leads to uniquely identified shocks up to ordering and sign. Hence, as long as one is willing to assume a single (time-varying) impact matrix, its columns characterize the estimated impact effects of the shocks, but it is not revealed which column is related to which shock. Because the impact matrix is also subject to estimation error, further constraints may be needed for labelling the shocks. The identification conditions are the same as in Virolainen (2022), however, and we repeat some of them for convenience.

The empirical application studies asymmetries in the expected effects of the monetary policy shock in the Euro area and considers a monthly data covering the period from January 1999 to December 2021. Our StMVAR model identifies two regimes: a low-growth regime and a high-growth regime. The low-growth regime is characterized by a negative (but volatile) output gap, and it mainly prevails after the collapse of Lehman Brothers in the Financial crisis but obtains large mixing weights also during and before the early 2000's recession. The high-growth regime is characterized by a positive output gap and it mainly dominates before the Financial crisis.

We find strong asymmetries with respect to the initial state of the economy and sign of the shock, but asymmetries with respect to the size of the shock are weak. The real effects are less enduring for an expansionary shock than for a contractionary shock. Particularly in the high-growth regime, a contractionary shock persistently drives the economy towards the low-growth regime, which translates to a very persistent decrease in the output gap. The inflationary effects of the monetary policy shock are stronger in the high-growth regime than in the low-growth regime, and in the latter the price level does not move much on average.

The rest of this paper is organized as follows. Section 2 introduces the linear Student's t VAR and establishes its stationary properties. Section 3 introduces the G-StMVAR model and discusses its properties. Section 4 introduces the structural G-StMVAR model and briefly discusses identification of the shocks. Section 5 discusses estimation of the model parameters by the method of max-

imum likelihood (ML) and establishes the asymptotic properties of the ML estimator. Section 6 discusses a strategy for building a G-StMVAR model, and Section 7 presents the empirical application to the asymmetric effects of the Euro area monetary policy shock. Appendix A provides the density functions and some properties of the Gaussian and Student's t distributions, Appendix B gives proofs for the stated theorems, and Appendix C provides details on the empirical application. Finally, this paper is accompanied with the CRAN distributed R package `gmvar` (Virolainen, 2018a) that provides tools for estimation and other numerical analysis of the models.

Throughout this paper, we use the following notation. We write $x = (x_1, \dots, x_n)$ for the column vector x where the components x_i may be either scalars or (column) vectors. The notation $x \sim n_d(\mu, \Sigma)$ signifies that the random vector x has a d -dimensional Gaussian distribution with mean μ and (positive definite) covariance matrix Σ , and $n_d(\cdot; \mu, \Sigma)$ denotes the corresponding density function. Similarly, $x \sim t_d(\mu, \Sigma, \nu)$ signifies that x has a d -dimensional t -distribution with mean μ , (positive definite) covariance matrix Σ , and degrees of freedom ν (assumed to satisfy $\nu > 2$), and $t_d(\cdot; \mu, \Sigma, \nu)$ denotes the corresponding density function. The vectorization operator vec stacks columns of a matrix on top of each other and $vech$ stacks them from the main diagonal downwards (including the main diagonal). The $(d \times d)$ identity matrix is denoted by I_d , \otimes denotes the Kronecker product, and $\mathbf{1}_d$ denotes a d -dimensional vectors of ones.

2 Linear Gaussian and Student's t vector autoregressions

The G-StMVAR model accommodates two types of mixture components: conditionally homoskedastic linear Gaussian vector autoregressions and conditionally heteroskedastic linear Student's t vector autoregressions. This section defines these linear vector autoregressions and establishes their stationary properties. Consider the d -dimensional linear VAR model defined as

$$z_t = \phi_0 + \sum_{i=1}^p A_i z_{t-i} + \Omega_t^{1/2} \varepsilon_t, \quad (2.1)$$

where the error process ε_t identically and independently distributed (IID), $\Omega_t^{1/2}$ is a symmetric square root matrix of the positive definite $(d \times d)$ covariance matrix Ω_t for all t , and $\phi_0 \in \mathbb{R}^d$. The $(d \times d)$ autoregression matrices are assumed to satisfy $\mathbf{A}_p \equiv [A_1 : \dots : A_p] \in \mathbb{S}^{d \times dp}$, where

$$\mathbb{S}^{d \times dp} = \{[A_1 : \dots : A_p] \in \mathbb{R}^{d \times dp} : \det(I_d - \sum_{i=1}^p A_i z^i) \neq 0 \text{ for } |z| \leq 1\} \quad (2.2)$$

defines the usual stability condition of a linear VAR. The linear Gaussian VAR is obtained from Equation (2.1) by assuming that ε_t follows the d -dimensional standard normal distribution and that the conditional covariance matrix is a constant, $\Omega_t = \Omega$. We will first establish the stationary properties of the linear Gaussian VAR, and by making use of the introduced notation, we then introduce the linear Student's t VAR.

Under the stability condition, the linear Gaussian VAR is stationary, and the following properties are obtained. Denoting $\mathbf{z}_t = (z_t, \dots, z_{t-p+1})$ and $\mathbf{z}_t^+ = (z_t, \mathbf{z}_{t-1})$, it is well known that the

stationary solution to (2.1) satisfies

$$\begin{aligned}
\mathbf{z}_t &\sim n_{dp}(\mathbf{1}_p \otimes \mu, \Sigma_p) \\
\mathbf{z}_t^+ &\sim n_{d(p+1)}(\mathbf{1}_{p+1} \otimes \mu, \Sigma_{p+1}) \\
z_t | \mathbf{z}_{t-1} &\sim n_d(\mu + \Sigma_{1p} \Sigma_p^{-1} (\mathbf{z}_{t-1} - \mathbf{1}_p \otimes \mu), \Sigma_1 - \Sigma_{1p} \Sigma_p^{-1} \Sigma_{1p}') = n_d(\phi_0 + \mathbf{A}_p \mathbf{z}_{t-1}, \Omega),
\end{aligned} \tag{2.3}$$

where the last line defines the conditional distribution of z_t given \mathbf{z}_{t-1} . Denoting by $\Sigma(h)$, $h = 0, \pm 1, \pm 2, \dots$, the lag h autocovariance matrix of z_t , the quantities $\mu, \Sigma_p, \Sigma_1, \Sigma_{1p}, \Sigma_{p+1}$ are given as (see, e.g., Lütkepohl, 2005, pp. 23, 28-29)

$$\begin{aligned}
\mu &= (I_d - \sum_{i=1}^p A_i)^{-1} \phi_0 && (d \times 1) \\
\text{vec}(\Sigma_p) &= (I_{(dp)^2} - \mathbf{A} \otimes \mathbf{A})^{-1} \text{vec}(\Omega) && ((dp)^2 \times 1) \\
\Sigma_1 &= \Sigma(0) && (d \times d) \\
\Sigma(p) &= A_1 \Sigma(p-1) + \dots + A_p \Sigma(0) && (d \times d) \\
\Sigma_{1p} &= [\Sigma(1) : \dots : \Sigma(p-1) : \Sigma(p)] = \mathbf{A}_p \Sigma_p && (d \times dp) \\
\Sigma_{p+1} &= \begin{bmatrix} \Sigma_1 & \Sigma_{1p} \\ \Sigma_{1p}' & \Sigma_p \end{bmatrix} && (d(p+1) \times d(p+1))
\end{aligned} \tag{2.4}$$

where

$$\Sigma_p = \begin{bmatrix} \Sigma(0) & \Sigma(1) & \dots & \Sigma(p-1) \\ \Sigma(-1) & \Sigma(0) & \dots & \Sigma(p-2) \\ \vdots & \vdots & \ddots & \vdots \\ \Sigma(-p+1) & \Sigma(-p+2) & \dots & \Sigma(0) \end{bmatrix}, \quad \Omega = \begin{bmatrix} \Omega & 0 & \dots & 0 \\ 0 & 0 & \dots & 0 \\ \vdots & \vdots & \ddots & \vdots \\ 0 & 0 & \dots & 0 \end{bmatrix}, \tag{2.5}$$

$(dp \times dp)$
 $(dp \times dp)$

and

$$\mathbf{A} = \begin{bmatrix} A_1 & A_2 & \dots & A_{p-1} & A_p \\ I_d & 0 & \dots & 0 & 0 \\ 0 & I_d & & 0 & 0 \\ \vdots & & \ddots & \vdots & \vdots \\ 0 & 0 & \dots & I_d & 0 \end{bmatrix}. \tag{2.6}$$

$(dp \times dp)$

In order to construct a linear Student's t VAR with stationary properties analogous to (2.3), we consider the appropriate marginal distribution of $p+1$ consecutive observations. Then, a connection to the VAR (2.1) is made through the conditional distribution, and finally this process and its stationary properties are formally established. Suppose that for a random vector in $\mathbb{R}^{d(p+1)}$ it holds that $(z, \mathbf{z}) \sim t_{d(p+1)}(\mathbf{1}_{p+1} \otimes \mu, \Sigma_{p+1}, \nu)$, where $\nu > 2$. By the properties of a multivariate Student's t -distribution (given in Appendix A), the conditional distribution of z given \mathbf{z} is $z | \mathbf{z} \sim t_d(\mu(\mathbf{z}), \Omega(\mathbf{z}), \nu + dp)$, where

$$\mu(\mathbf{z}) = \phi_0 + \mathbf{A}_p \mathbf{z} \tag{2.7}$$

$$\Omega(\mathbf{z}) = \frac{\nu - 2 + (\mathbf{z} - \mathbf{1}_p \otimes \mu)' \Sigma_p^{-1} (\mathbf{z} - \mathbf{1}_p \otimes \mu)}{\nu - 2 + dp} \Omega. \tag{2.8}$$

It is easy to see that a VAR of the form (2.1) that has the above-described conditional Student's t -distribution is obtained by assuming that $\varepsilon_t \sim t_d(0, I_d, \nu + dp)$ and that the conditional covariance matrix Ω_t is of the form (2.8). The following theorem then formally establishes this Student's t VAR and its stationary properties (which is analogous to Theorem 1 in Meitz *et al.*, forthcoming, considering a univariate version of the Student's t autoregression).

Theorem 1. *Suppose $\phi_0 \in \mathbb{R}^d$, $[A_1 : \dots : A_p] \in \mathbb{S}^{d \times dp}$, $\Omega \in \mathbb{R}^{d \times d}$ is positive definite, and that $\nu > 2$. Then, there exists a process $\mathbf{z}_t = (z_t, \dots, z_{t-p+1})$ ($t = 0, 1, 2, \dots$) with the following properties.*

- (i) *The process \mathbf{z}_t is a Markov chain on \mathbb{R}^{dp} with a stationary distribution characterized by the density function $t_{dp}(\mathbf{1}_p \otimes \mu, \Sigma_p, \nu)$. When $\mathbf{z}_0 \sim t_{dp}(\mathbf{1}_p \otimes \mu, \Sigma_p, \nu)$, we have, for $t = 1, 2, \dots$, that $\mathbf{z}_t^+ \sim t_{d(p+1)}(\mathbf{1}_{p+1} \otimes \mu, \Sigma_{p+1}, \nu)$ and the conditional distribution of z_t given \mathbf{z}_{t-1} is*

$$z_t | \mathbf{z}_{t-1} \sim t_d(\mu(\mathbf{z}_{t-1}), \Omega(\mathbf{z}_{t-1}), \nu + dp). \quad (2.9)$$

- (ii) *Furthermore, for $t = 1, 2, \dots$, the process z_t has the representation*

$$z_t = \phi_0 + \sum_{i=1}^p A_i z_{t-i} + \Omega_t^{1/2} \varepsilon_t, \quad (2.10)$$

where $\Omega_t = \Omega(\mathbf{z}_{t-1})$ is the conditional covariance matrix (see (2.8)), $\varepsilon_t \sim \text{IID } t_d(0, I_d, \nu + dp)$, and ε_t are independent of $\{z_{t-j}, j > 0\}$ for all t .

Analogously to the univariate linear Student's autoregression discussed in Meitz *et al.* (forthcoming), the results (i) and (ii) in Theorem 1 are comparable to properties (2.3) and (2.1) of the Gaussian counterpart. Part (i) shows that both the stationary and conditional distributions of z_t are t -distributions, whereas part (ii) clarifies the connection to the standard VAR model.

Our Student's t VAR has a conditional mean identical to the Gaussian VAR, but unlike the Gaussian VAR, it is conditionally heteroskedastic. Specifically, the conditional variance (2.8) consists of a constant covariance matrix that is multiplied by a time-varying scalar that depends on the quadratic form of the preceding p observations through the autoregressive parameters. In this sense, the model has a 'VAR(p)–ARCH(p)' representation, but the ARCH type conditional variance is not as general as in the conventional multivariate ARCH process (e.g., Lütkepohl, 2005, Section 16.3) that allows the entries of the conditional covariance matrix to vary relative to each other. Our model is, however, more parsimonious than the conventional VAR-ARCH model, as the conditional covariance depends only on the degrees of freedom and autoregressive parameters (in addition to the parameters in the constant covariance matrix). Student's t VARs similar to ours have previously appeared at least in Heracleous (2003) and Poudyal (2012).

3 The Gaussian and Student's t mixture vector autoregressive model

The G-StMVAR model can be described as a collection of linear autoregressive models that are the linear Gaussian VARs or the linear Student's t VARs defined in Section 2. At each time point, the process generates an observation from one of its mixture components that is randomly selected according to the probabilities given by the mixing weights. This definition is formalized next.

Let y_t ($t = 1, 2, \dots$) be the real valued d -dimensional time series of interest, and let \mathcal{F}_{t-1} denote σ -algebra generated by the random vectors $\{y_s, s < t\}$. In a G-StMVAR model with autoregressive order p and M mixture components (or regimes), the observations y_t are assumed to be generated by

$$y_t = \sum_{m=1}^M s_{m,t} (\mu_{m,t} + \Omega_{m,t}^{1/2} \varepsilon_{m,t}), \quad (3.1)$$

$$\mu_{m,t} = \phi_{m,0} + \sum_{i=1}^p A_{m,i} y_{t-i}, \quad (3.2)$$

where the following conditions hold (which are similar to Condition 1 in Kalliovirta *et al.*, 2016).

Condition 1.

- (a) For $m = 1, \dots, M_1 \leq M$, the random vectors $\varepsilon_{m,t}$ are IID $n_d(0, I_d)$ distributed, and for $m = M_1 + 1, \dots, M$, they are IID $t_d(0, I_d, \nu_m + dp)$ distributed. For all m , $\varepsilon_{m,t}$ are independent of \mathcal{F}_{t-1} .
- (b) For each $m = 1, \dots, M$, $\phi_{m,0} \in \mathbb{R}^d$, $\mathbf{A}_{m,p} \equiv [A_{m,1} : \dots : A_{m,p}] \in \mathbb{S}^{d \times dp}$ (the set $\mathbb{S}^{d \times dp}$ is defined in (2.2)), and Ω_m is positive definite. For $m = 1, \dots, M_1$, the conditional covariance matrices are constants, $\Omega_{m,t} = \Omega_m$. For $m = M_1 + 1, \dots, M$, the conditional covariance matrices $\Omega_{m,t}$ are as in (2.8), except that \mathbf{z} is replaced with $\mathbf{y}_{t-1} = (y_{t-1}, \dots, y_{t-p})$ and the regime specific parameters $\phi_{m,0}, \mathbf{A}_{m,p}, \Omega_m, \nu_m$ are used to define the quantities therein. For $m = M_1 + 1, \dots, M$, also $\nu_m > 2$.
- (c) The unobservable regime variables $s_{1,t}, \dots, s_{M,t}$ are such that at each t , exactly one of them takes the value one and the others take the value zero according to the conditional probabilities expressed in terms of the (\mathcal{F}_{t-1} -measurable) mixing weights $\alpha_{m,t} \equiv P(s_{m,t} = 1 | \mathcal{F}_{t-1})$ that satisfy $\sum_{m=1}^M \alpha_{m,t} = 1$.
- (d) Conditionally on \mathcal{F}_{t-1} , $(s_{1,t}, \dots, s_{M,t})$ and $\varepsilon_{m,t}$ are assumed independent.

The conditions $\nu_m > 2$ in (b) are made to ensure the existence of second moments. This definition implies that the G-StMVAR model generates each observation from one of its mixture components, a linear Gaussian or Student's t vector autoregression discussed in Section 2, and that the mixture component is selected randomly according to the probabilities given by the mixing weights $\alpha_{m,t}$.

The first M_1 mixture components are assumed to be linear Gaussian VARs, and the last $M_2 \equiv M - M_1$ mixture components are assumed to be linear Student's t VARs. If all the component

processes are Gaussian VARs ($M_1 = M$), the G-StMVAR model reduces to the GMVAR model of Kalliovirta *et al.* (2016). If all the component processes are Student's t VARs ($M_1 = 0$), we refer to the model as the StMVAR model.

Equations (3.1) and (3.2) and Condition 1 lead to a model in which the conditional density function of y_t conditional on its past, \mathcal{F}_{t-1} , is given as

$$f(y_t | \mathcal{F}_{t-1}) = \sum_{m=1}^{M_1} \alpha_{m,t} n_d(y_t; \mu_{m,t}, \Omega_m) + \sum_{m=M_1+1}^M \alpha_{m,t} t_d(y_t; \mu_{m,t}, \Omega_{m,t}, \nu_m + dp). \quad (3.3)$$

The conditional densities $n_d(y_t; \mu_{m,t}, \Omega_{m,t})$ are obtained from (2.3), whereas $t_d(y_t; \mu_{m,t}, \Omega_{m,t}, \nu_m + dp)$ are obtained from Theorem 1. The explicit expressions of the density functions are given in Appendix A. To fully define the G-StMVAR model it is then left to specify the mixing weights.

Analogously to Kalliovirta *et al.* (2015), Kalliovirta *et al.* (2016), Meitz *et al.* (forthcoming), and Virolainen (forthcoming), we define the mixing weights as weighted ratios of the component process stationary densities corresponding to the previous p observations. In order to formally specify the mixing weights, we first define the following function for notational convenience. Let

$$d_{m,dp}(\mathbf{y}; \mathbf{1}_p \otimes \mu_m, \Sigma_{m,p}, \nu_m) = \begin{cases} n_{dp}(\mathbf{y}; \mathbf{1}_p \otimes \mu_m, \Sigma_{m,p}), & \text{when } m \leq M_1, \\ t_{dp}(\mathbf{y}; \mathbf{1}_p \otimes \mu_m, \Sigma_{m,p}, \nu_m), & \text{when } m > M_1, \end{cases} \quad (3.4)$$

where the dp -dimensional densities $n_{dp}(\mathbf{y}; \mathbf{1}_p \otimes \mu_m, \Sigma_{m,p})$ and $t_{dp}(\mathbf{y}; \mathbf{1}_p \otimes \mu_m, \Sigma_{m,p}, \nu_m)$ correspond to the stationary distribution of the m th component process (given in Equation (2.3) for the Gaussian regimes and in Theorem 1 for the Student's t regimes). Denoting $\mathbf{y}_{t-1} = (y_{t-1}, \dots, y_{t-p})$, the mixing weights of the G-StMVAR model are defined as

$$\alpha_{m,t} = \frac{\alpha_m d_{m,dp}(\mathbf{y}_{t-1}; \mathbf{1}_p \otimes \mu_m, \Sigma_{m,p}, \nu_m)}{\sum_{n=1}^M \alpha_n d_{n,dp}(\mathbf{y}_{t-1}; \mathbf{1}_p \otimes \mu_n, \Sigma_{n,p}, \nu_n)}, \quad (3.5)$$

where $\alpha_m \in (0, 1)$, $m = 1, \dots, M$, are mixing weights parameters assumed to satisfy $\sum_{m=1}^M \alpha_m = 1$, $\mu_m = (I_d - \sum_{i=1}^p A_{m,i})^{-1} \phi_{m,0}$, and covariance matrix $\Sigma_{m,p}$ is given in (2.4), (2.5), and (2.6) but using the regime specific parameters to define the quantities therein.

Because the mixing weights are weighted ratios of the component process stationary densities corresponding to the previous p observations, the greater the relative weighted likelihood of a regime is, the more likely the process generates an observation from it. This is a convenient feature for forecasting, and it also facilitates associating statistical characteristics and economic interpretations to the regimes. Moreover, it turns out that this specific formulation of the mixing weights leads to attractive theoretical properties such as full knowledge of the stationary distribution of $p + 1$ consecutive observations and ergodicity of the process. These properties are summarized in the following theorem.

Before stating the theorem, a few notational conventions are provided. We collect the parameters of a G-StMVAR model to the $((M(d + d^2p + d(d + 1)/2 + 2) - M_1 - 1) \times 1)$ vector $\boldsymbol{\theta} = (\boldsymbol{\vartheta}_1, \dots, \boldsymbol{\vartheta}_M, \alpha_1, \dots, \alpha_{M-1}, \boldsymbol{\nu})$, where $\boldsymbol{\vartheta}_m = (\phi_{m,0}, \text{vec}(\mathbf{A}_{m,p}), \text{vech}(\Omega_m))$ and $\boldsymbol{\nu} = (\nu_{M_1+1}, \dots, \nu_M)$. The last mixing weight parameter α_M is not parametrized because it is obtained from the restriction $\sum_{m=1}^M \alpha_m = 1$. The G-StMVAR model with autoregressive order p , and M_1 Gaussian and M_2

Student's t mixture components is referred to as the G-StMVAR(p, M_1, M_2) model, whenever the order of the model needs to be emphasized.

Theorem 2. *Consider the G-StMVAR process y_t generated by (3.1), (3.2), and (3.5) with Condition 1 satisfied. Then, $\mathbf{y}_t = (y_t, \dots, y_{t-p+1})$ is a Markov chain on \mathbb{R}^{dp} with stationary distribution characterized by the density*

$$f(\mathbf{y}; \boldsymbol{\theta}) = \sum_{m=1}^{M_1} \alpha_m n_{dp}(\mathbf{y}; \mathbf{1}_p \otimes \mu_m, \Sigma_{m,p}) + \sum_{m=M_1+1}^M \alpha_m t_{dp}(\mathbf{y}; \mathbf{1}_p \otimes \mu_m, \Sigma_{m,p}, \nu_m). \quad (3.6)$$

Moreover, \mathbf{y}_t is ergodic.

The stationary distribution is a mixture of M_1 dp -dimensional Gaussian distributions and M_2 dp -dimensional t -distributions with constant mixing weights α_m . The proof of Theorem 2 in Appendix B shows that the marginal stationary distributions of $1, \dots, p+1$ consecutive observations are likewise mixtures of Gaussian and t -distributions. This gives the mixing weight parameters $\alpha_m, m = 1, \dots, M$, interpretation as the unconditional probabilities of an observation being generated from the m th component process. The unconditional mean, covariance, and first p autocovariances are hence obtained as $E[y_t] = \sum_{m=1}^M \alpha_m \mu_m$ and

$$\text{Cov}(y_t, y_{t-j}) = \sum_{m=1}^M \alpha_m \Sigma_m(j) + \sum_{m=1}^M \alpha_m (\mu_m - E[y_t]) (\mu_m - E[y_t])', \quad (3.7)$$

where $j = 0, 1, \dots, p$ and $\Sigma_m(j)$ is the j th autocovariance matrix of the m th component process.

The conditional mean of the G-StMVAR process can be expressed as $E[y_t | \mathcal{F}_{t-1}] = \sum_{m=1}^M \alpha_{m,t} \mu_{m,t}$ and the conditional covariance matrix as

$$\text{Cov}(y_t | \mathcal{F}_{t-1}) = \sum_{m=1}^M \alpha_{m,t} \Omega_{m,t} + \sum_{m=1}^M \alpha_{m,t} (\mu_{m,t} - E[y_t | \mathcal{F}_{t-1}]) (\mu_{m,t} - E[y_t | \mathcal{F}_{t-1}])'. \quad (3.8)$$

The conditional mean is a weighted sum of the component process conditional means. The conditional variance consists of two terms. The first term is a weighted sum of the component process conditional covariance matrices, and the second term captures conditional heteroskedasticity caused by variations in the conditional mean.

By construction, the StMVAR model does not generally filter out autocorrelation as well as its Gaussian counterpart, the GMVAR model (Kalliovirta *et al.*, 2016), because the autoregressive parameters are also the coefficients for ARCH type conditional heteroskedasticity. This property arises from the utilization of the multivariate Student's t -distribution as the stationary distribution of the component processes. The utilization of the t -distribution allows for parsimonious modelling of series that display fat tails and conditional heteroskedasticity within the regimes. This is particularly advantageous in the context of mixture VARs, as the large number of parameters may often be a problem even without an ARCH component. Appropriate modelling of kurtosis and conditional heteroskedasticity is important, since they may affect the endogenously determined

regime-switching probabilities. Ignoring the modelling of kurtosis and conditional heteroskedasticity would leave out potentially important dynamics that may affect the outcome of an empirical investigation. If some of the regimes have a constant conditional covariance matrix and zero excess kurtosis, we allow them to be conditionally homoskedastic linear Gaussian VARs, which leads to the G-StMVAR model.

4 Structural G-StMVAR model

4.1 The model setup

The G-StMVAR model can be extended to a structural version similarly to the structural GMVAR model discussed in Virolainen (2022).¹ Consider the G-StMVAR model defined by (3.1), (3.2), and (3.5) with Condition 1 satisfied. We write the structural G-StMVAR model as

$$y_t = \sum_{m=1}^M s_{m,t} (\phi_{m,0} + \sum_{i=1}^p A_{m,i} y_{t-i}) + B_t e_t, \quad (4.1)$$

$$u_t \equiv B_t e_t = \sum_{m=1}^M s_{m,t} \Omega_{m,t}^{1/2} \varepsilon_{m,t}, \quad (4.2)$$

where e_t ($d \times 1$) is an orthogonal structural error. This definition is similar to Equations (3.1) and (3.2) in Virolainen (2022) but with Student's t regimes in addition to the Gaussian ones.

For the Gaussian regimes ($m = 1, \dots, M_1$), $\Omega_{m,t} = \Omega_m$. For the Student's t regimes ($m = M_1 + 1, \dots, M$), $\Omega_{m,t} = \omega_{m,t} \Omega_m$, where

$$\omega_{m,t} = \frac{\nu_m - 2 + (\mathbf{y}_{t-1} - \mathbf{1}_p \otimes \mu_m)' \Sigma_{m,p}^{-1} (\mathbf{y}_{t-1} - \mathbf{1}_p \otimes \mu_m)}{\nu_m - 2 + dp}. \quad (4.3)$$

The invertible ($d \times d$) "B-matrix" B_t , which governs the contemporaneous relationships of the shocks, is time-varying and a function of y_{t-1}, \dots, y_{t-p} . We will define the B-matrix so that it captures the conditional heteroskedasticity of the reduced form error, and thereby amplifies a constant-sized structural shock accordingly. Appropriate modelling of conditional heteroskedasticity in the B-matrix is of interest because the (generalized) impulse response functions may be asymmetric with respect to the size of the shock.

We have $\Omega_{u,t} \equiv \text{Cov}(u_t | \mathcal{F}_{t-1}) = \sum_{m=1}^{M_1} \alpha_{m,t} \Omega_m + \sum_{m=M_1+1}^M \alpha_{m,t} \omega_{m,t} \Omega_m$, while the conditional covariance matrix of the structural error $e_t = B_t^{-1} u_t$ (which are not IID but martingale differences and thereby uncorrelated) is obtained as

$$\text{Cov}(e_t | \mathcal{F}_{t-1}) = \sum_{m=1}^{M_1} \alpha_{m,t} B_t^{-1} \Omega_m B_t'^{-1} + \sum_{m=M_1+1}^M \alpha_{m,t} \omega_{m,t} B_t^{-1} \Omega_m B_t'^{-1}. \quad (4.4)$$

¹ The structural GMVAR model of Virolainen (2022) is obtained as special case of our model by selecting $M_1 = M$, i.e., that all the regimes are of the GMVAR type.

Therefore, the B-matrix should be chosen so that the structural shocks are orthogonal regardless of which regime they come from. Virolainen (2022) shows that any such B-matrix has (linearly independent) eigenvectors of the matrix $\Omega_m \Omega_1^{-1}$ as its columns. Moreover, he shows that under the following assumption and a constant normalization of the structural error's conditional variance, say, $\Omega_{u,t} = I_d$, the B-matrix is unique up to ordering of its columns and changing all signs in a column.²

Assumption 1. Consider M positive definite $(d \times d)$ covariance matrices Ω_m , $m = 1, \dots, M$, and denote the strictly positive eigenvalues of the matrices $\Omega_m \Omega_1^{-1}$ as λ_{mi} , $i = 1, \dots, d$, $m = 2, \dots, M$. Suppose that for all $i \neq j \in \{1, \dots, d\}$, there exists an $m \in \{2, \dots, M\}$ such that $\lambda_{mi} \neq \lambda_{mj}$.

Thus, as long as one is willing to assume a single (time-varying) B-matrix, its columns generally characterize the estimated impact effects of the shocks, but it is not revealed which column is related to which shock. Since the B-matrix is also subject to estimation error, further constraints may be needed for labelling the shocks.

Following Virolainen (2022) (and Lanne and Lütkepohl (2010) and Lanne, Lütkepohl, and Maciejowska (2010)), we utilize the following matrix decomposition that is convenient for specifying the B-matrix and deriving the identification conditions. We decompose the error term covariance matrices as

$$\Omega_1 = WW' \quad \text{and} \quad \Omega_m = W\Lambda_m W', \quad m = 2, \dots, M, \quad (4.5)$$

where the diagonal of $\Lambda_m = \text{diag}(\lambda_{m1}, \dots, \lambda_{md})$, $\lambda_{mi} > 0$ ($i = 1, \dots, d$), contains the eigenvalues of the matrix $\Omega_m \Omega_1^{-1}$ and the columns of the nonsingular W are the related eigenvectors (that are the same for all m by construction). When $M = 2$, decomposition (4.5) always exists (Muirhead, 1982, Theorem A9.9), but for $M \geq 3$ its existence requires that the matrices $\Omega_m \Omega_1^{-1}$ share the common eigenvectors in W . If this is not the case, the B-matrix does not exist (see Virolainen, 2022, Section 3.1), but its existence is, however, testable.

Similarly to Virolainen (2022), any scalar multiples of W 's columns comprise an appropriate B-matrix, but only specific scalar multiples comprise the locally unique B-matrix associated with a given normalization of the structural error's conditional covariance matrix. Direct calculation shows that the B-matrix associated with the normalization $\text{Cov}(e_t | \mathcal{F}_{t-1}) = I_d$ is obtained as

$$B_t = W \left(\sum_{m=1}^{M_1} \alpha_{m,t} \Lambda_m + \sum_{m=M_1+1}^M \alpha_{m,t} \omega_{m,t} \Lambda_m \right)^{1/2}, \quad (4.6)$$

where $B_t B_t' = \Omega_{u,t}$. Since $B_t^{-1} \Omega_m B_t'^{-1} = \Lambda_m (\sum_{n=1}^{M_1} \alpha_{n,t} \Lambda_n + \sum_{n=M_1+1}^M \alpha_{n,t} \omega_{n,t} \Lambda_n)^{-1}$, the B-matrix (4.6) simultaneously diagonalizes $\Omega_1, \dots, \Omega_M$, and $\Omega_{u,t}$ (and thereby also $\Omega_{1,t}, \dots, \Omega_{M,t}$) for each t so that $\text{Cov}(e_t | \mathcal{F}_{t-1}) = I_d$.

² Virolainen (2022) shows the uniqueness of the B-matrix for the structural GMVAR model, but the results apply to our structural G-StMVAR model as well.

4.2 Identification of the shocks

We have established that in the model defined by (4.1) and (4.2) with the normalization $\text{Cov}(e_t|\mathcal{F}_{t-1}) = I_d$, the structural shocks are identified up ordering and sign under Assumption 1. Global statistical identification of the shocks is therefore obtained by fixing the signs and ordering of the columns of B_t . The ordering of the columns can be fixed by fixing an arbitrary ordering for the eigenvalues in the diagonals of Λ_m , $m = 2, \dots, M$. The signs, in turn, can be normalized by placing a single strict sign constraint in each column of B_t .

However, the interest is often in identifying some specific shock (or shocks). To that end, the correct structural shock needs to be uniquely related to the shock of interest through constraints on the B-matrix (or equally W) that only the shock of interest satisfies. Virolainen (2022, Proposition 2) gives formal conditions for global identification of any subset of the shocks when the relevant pairs eigenvalues λ_{mi} are distinct in some regime. He also derives conditions for globally identifying some of the shocks when one of the relevant pairs of the eigenvalues is identical in all regimes (Virolainen, 2022, Proposition 3). For convenience, we repeat the conditions in the former case below, but in the latter case (as well as for the proof of the proposition below), we refer to Virolainen (2022).

Proposition 1. *Suppose $\Omega_1 = WW'$ and $\Omega_m = W\Lambda_mW'$, $m = 2, \dots, M$, where $\Lambda_m = \text{diag}(\lambda_{m1}, \dots, \lambda_{md})$, $\lambda_{mi} > 0$ ($i = 1, \dots, d$), contains the eigenvalues of $\Omega_m\Omega_1^{-1}$ in the diagonal and the columns of the nonsingular W are the related eigenvectors. Then, the last d_1 structural shocks are uniquely identified if*

- (1) *for all $j > d - d_1$ and $i \neq j$ there exists an $m \in \{2, \dots, M\}$ such that $\lambda_{mi} \neq \lambda_{mj}$,*
- (2) *the columns of W are constrained in a way that for all $i \neq j > d - d_1$, the i th column cannot satisfy the constraints of the j th column as is nor after changing all signs in the i th column, and*
- (3) *there is at least one (strict) sign constraint in each of the last d_1 columns of W .*

Condition (3) fixes the signs in the last d_1 columns of W , and therefore the signs of the instantaneous effects of the corresponding shocks. However, since changing the signs of the columns is effectively the same as changing the signs of the corresponding shocks, and the structural shock has a distribution that is symmetric about zero, this condition is not restrictive. The assumption that the last d_1 shocks are identified is not restrictive either, as one may always reorder the structural shocks accordingly. See Virolainen (2022) for examples on identifying shocks with this proposition. Finally, note that Assumption 1 is not required for identification, when only some of the shocks are to be identified. In that case, it is replaced with the weaker Condition (1) (that is always satisfied under Assumption 1). If Condition (1) is strengthened to Assumption 1, the model is statistically identified and the constraints imposed in Condition (2) become testable. If Assumption 1 is not satisfied, the testing problem is nonstandard and the conventional asymptotic distributions of likelihood ratio and Wald test statistics are unreliable (see the discussion in Virolainen, 2022).

5 Estimation

The parameters of the G-StMVAR model can be estimated by the method of maximum likelihood (ML). Even the exact log-likelihood function is available, as we have established the stationary distribution of the process in Theorem 2. Suppose the observed time series is $y_{-p+1}, \dots, y_0, y_1, \dots, y_T$ and that the initial values are stationary. Then, the log-likelihood function of the G-StMVAR model takes the form

$$L(\boldsymbol{\theta}) = \log \left(\sum_{m=1}^M \alpha_m d_{m,dp}(\mathbf{y}_0; \mathbf{1}_p \otimes \boldsymbol{\mu}_m, \boldsymbol{\Sigma}_{m,p}, \nu_m) \right) + \sum_{m=1}^M l_t(\boldsymbol{\theta}), \quad (5.1)$$

where $d_{m,dp}(\cdot; \mathbf{1}_p \otimes \boldsymbol{\mu}_m, \boldsymbol{\Sigma}_{m,p}, \nu_m)$ is defined in (3.4) and

$$l_t(\boldsymbol{\theta}) = \log \left(\sum_{m=1}^{M_1} \alpha_{m,t} n_d(y_t; \boldsymbol{\mu}_{m,t}, \Omega_m) + \sum_{m=M_1+1}^M \alpha_{m,t} t_d(y_t; \boldsymbol{\mu}_{m,t}, \Omega_{m,t}, \nu_m + dp) \right). \quad (5.2)$$

If stationarity of the initial values seems unreasonable, one can condition on the initial values and base the estimation on the conditional log-likelihood function, which is obtained by dropping the first term on the right side of (5.1). The rest of this section assumes that estimation is based on the conditional log-likelihood function divided by the sample size, $L_T^{(c)}(\boldsymbol{\theta}) = T^{-1} \sum_{m=1}^M l_t(\boldsymbol{\theta})$, i.e., the ML estimator $\hat{\boldsymbol{\theta}}_T$ maximizes $L_T^{(c)}(\boldsymbol{\theta})$.

If there are two regimes in the model ($M = 2$), the structural G-StMVAR model is obtained from the estimated reduced form model by decomposing the covariance matrices $\Omega_1, \dots, \Omega_M$ as in (4.5). If $M \geq 3$ or overidentifying constraints are imposed on B_t through W , the model can be reparametrized with W and Λ_m ($m = 2, \dots, M$) instead of $\Omega_1, \dots, \Omega_M$, and the log-likelihood function can be maximized subject to the new set of parameters and constraints. In this case, the decomposition (4.5) is plugged in to the log-likelihood function and $\text{vech}(\Omega_1), \dots, \text{vech}(\Omega_M)$ are replaced with $\text{vec}(W)$ and $\boldsymbol{\lambda}_2, \dots, \boldsymbol{\lambda}_M$ in the parameter vector $\boldsymbol{\theta}$, where $\boldsymbol{\lambda}_m = (\lambda_{m1}, \dots, \lambda_{md})$. Instead of constraining $\text{vech}(\Omega_1), \dots, \text{vech}(\Omega_M)$ so that $\Omega_1, \dots, \Omega_M$ are positive definite, we impose the constraints $\lambda_{mi} > 0$ for all $m = 2, \dots, M$ and $i = 1, \dots, d$.

Establishing the asymptotic properties of the ML estimator requires that it is uniquely identified. In order to achieve unique identification, the parameters need to be constrained so that the mixture components cannot be 'relabelled' to produce the same model with a different parameter vector. The required assumption is

$$\alpha_1 > \dots > \alpha_{M_1} > 0, \alpha_{M_1+1} > \dots > \alpha_M > 0, \text{ and } \boldsymbol{\vartheta}_i = \boldsymbol{\vartheta}_j \text{ only if any of the conditions} \quad (5.3)$$

(1) $1 \leq i = j \leq M$, (2) $i \leq M_1 < j$, (3) $i, j > M_1$ and $\nu_i \neq \nu_j$, is satisfied.

In the case of the structural G-StMVAR model, identification also requires that Assumption 1 is satisfied (see Section 4).³ Then, identification of the structural model follows from the identification of the reduced form model.

We summarize the constraints imposed on the parameter space in the following assumption.

³ With the appropriate zero constraints on W , this condition can be relaxed, however (see the related discussion in Virolainen, 2022).

Assumption 2. *The true parameter value θ_0 is an interior point of Θ , which is a compact subset of $\{\theta = (\vartheta_1, \dots, \vartheta_M, \alpha_1, \dots, \alpha_{M-1}, \nu) \in \mathbb{R}^{M(d+d^2p+d(d+1)/2)} \times (0, 1)^{M-1} \times (2, \infty)^{M_2} : \mathbf{A}_{m,p} \in \mathbb{S}^{d \times dp}, \Omega_m \text{ is positive definite, for all } m = 1, \dots, M, \text{ and (5.3) holds}\}$.*

Asymptotic properties of the ML estimator under the conventional high-level conditions are stated in the following theorem. Denote $\mathcal{I}(\theta) = E \left[\frac{\partial l_t(\theta)}{\partial \theta} \frac{\partial l_t(\theta)}{\partial \theta'} \right]$ and $\mathcal{J}(\theta) = E \left[\frac{\partial^2 l_t(\theta)}{\partial \theta \partial \theta'} \right]$.

Theorem 3. *Suppose that y_t are generated by the stationary and ergodic G-StMVAR process of Theorem 2 and that Assumption 2 holds. Then, $\hat{\theta}_T$ is strongly consistent, i.e., $\hat{\theta}_T \rightarrow \theta_0$ almost surely. Suppose further that (i) $T^{1/2} \frac{\partial}{\partial \theta_0} L_T^{(c)}(\theta_0) \xrightarrow{d} N(0, \mathcal{I}(\theta_0))$ with $\mathcal{I}(\theta_0)$ finite and positive definite, (ii) $\mathcal{J}(\theta_0) = -\mathcal{I}(\theta_0)$, and (iii) $E[\sup_{\theta \in \Theta_0} |\frac{\partial^2 l_t(\theta)}{\partial \theta \partial \theta'}|] < \infty$ for some Θ_0 , compact convex set contained in the interior of Θ that has θ_0 as an interior point. Then $T^{1/2}(\hat{\theta}_T - \theta_0) \xrightarrow{d} N(0, -\mathcal{J}(\theta_0)^{-1})$.*

Given consistency, conditions (i)-(iii) of Theorem 3 are standard for establishing asymptotic normality of the ML estimator, but their verification can be tedious. If one is willing to assume the validity of these conditions, the ML estimator has the conventional limiting distribution, implying that the approximate standard errors for the estimates are obtained as usual. Furthermore, the standard likelihood based tests are applicable as long as the number of mixture components is correctly specified.⁴

Finding the ML estimate amounts to maximizing the log-likelihood function defined in (5.1) and (5.2) over a high dimensional parameter space satisfying the constraints summarized in Assumption 2. Due to the complexity of the log-likelihood function, numerical optimization methods are required. The maximization problem can be challenging in practice due to the mixing weights' complex dependence on the preceding observations, which induces a large number of modes to the surface of the log-likelihood function, and large areas to the parameter space, where it is flat in multiple directions. Also, the popular EM algorithm (Redner and Walker, 1984) is virtually useless here, as at each maximization step one faces a new optimization problem that is not much simpler than the original one. Following Meitz, Preve, and Saikkonen (2018), Meitz *et al.* (forthcoming) and Virolainen (2018a,b, forthcoming), we therefore employ a two-phase estimation procedure in which a genetic algorithm is used to find starting values for a gradient based method. The R package gmvarkit (Virolainen, 2018a) that accompanies this paper employs a modified genetic algorithm that works similarly to the one described in Virolainen (forthcoming).

⁴ This condition is important, because if the number of Gaussian or Student's t type mixture components is chosen too large, some of the parameters are not identified causing the result of Theorem 3 to break down. This particularly happens when one tests for the number of regimes, as under the null some of the regimes are removed from the model. Meitz and Saikkonen (2021) have, however, recently developed such tests for mixture autoregressive models with Gaussian conditional densities. Developing a test for the number of a regimes in the G-StMVAR model is a major task and beyond the scope of this paper. Likewise, when testing whether a regime is a Gaussian VAR against the alternative that it is a Student's t VAR, under the null, $\nu_m = \infty$ for the Student's t regime m to be tested, which violates Assumption 2.

6 Building a G-StMVAR model

Building a G-StMVAR model amounts to finding a suitable autoregressive order p , the number of Gaussian regimes M_1 , and the number of Student's t regimes M_2 . We propose a model selection strategy that takes advantage of the observation that the G-StMVAR model is a limiting case of the StMVAR model (in which all the mixture components are linear Student's t VARs).

It is easy to check that the linear Gaussian vector autoregression defined in Section 2 is a limiting case of the linear Student's t vector autoregression when the degrees of freedom parameter tends to infinity. As the mixing weights (3.5) are weighted ratios of the component process stationary densities, it then follows that a G-StMVAR(p, M_1, M_2) model is obtained as a limiting case of the StMVAR(p, M) model (or equivalently the G-StMVAR($p, 0, M$) model) with the degrees of freedom parameters of the first M_1 regimes tending to infinity. Since a StMVAR(p, M) model that is fitted to data generated by a G-StMVAR(p, M_1, M_2) process is, therefore, asymptotically expected to get large estimates for the degrees of freedom parameters of the first M_1 regimes, we propose starting model selection by finding a suitable StMVAR model. If the StMVAR model contains overly large degrees of freedom parameter estimates, one should switch the corresponding regimes to Gaussian VARs by estimating the appropriate G-StMVAR model.

For a strategy to find a suitable StMVAR model, we follow Kalliovirta *et al.* (2015), and suggest first considering the linear version of the model, that is, a StMVAR model with one mixture component. Partial autocorrelation functions, information criteria, and quantile residual diagnostics (see Kalliovirta and Saikkonen, 2010) may be made use of as usual for selecting the appropriate autoregressive order p . If the linear model is found inadequate, mixture versions of the model can be examined. One should, however, be conservative with the choice of M , because if the number of regimes is chosen too large, some of the parameters are not identified. Adding new regimes to the model also vastly increases the number of parameters, and moreover, due to the increased complexity, it might be difficult to obtain the ML estimate if there are many regimes in the model.

Overly large degrees of freedom parameters are redundant in the model, but their weak identification also causes numerical problems. Specifically, they induce a numerically nearly singular Hessian matrix of the log-likelihood function when evaluated at the estimate, which makes the approximate standard errors and the quantile residual diagnostic tests of Kalliovirta and Saikkonen (2010) often unavailable. Since removal of overly large degrees of freedom parameters by switching to the appropriate G-StMVAR model has little effect on the model's fit, the switch is advisable whenever overly large degrees of freedom parameter estimates are obtained.

7 Empirical application

As an empirical application, we study asymmetries in the expected effects of the monetary policy shock in the Euro area. Asymmetric effects of the Euro area monetary policy shock have been studied, among others, by Peersman and Smets (2002) and Dolado and María-Dolores (2006), who found that monetary policy shock has larger effects on production during recessions than

expansions. Pellegrino (2018) found real effects of the monetary policy shock weaker during uncertain times than tranquil times, whereas Burgard *et al.* (2019) found the effects of contractionary monetary policy shocks stronger but less enduring during "crisis" than during "normal times".

We consider a monthly Euro area data covering the period from January 1999 to December 2021 (276 observations) and consisting of four variables: industrial production index (IPI), harmonized consumer price index (HCPI), Brent crude oil price (Europe, OIL), and an interest rate variable (RATE). Our policy variable is the interest rate variable, which is the Euro overnight index average (EONIA) from January 1999 to October 2008 and the Wu and Xia (2016) shadow rate from November 2008 to December 2021. The Wu and Xia (2016) shadow rate is a shadow interest rate that is not bounded by the zero-lower-bound and also quantifies unconventional monetary policy measures.⁵ Overall, our empirical application closely resembles that of Virolainen (2022), who studied asymmetries in the expected effects of monetary policy shocks in the U.S. in a structural GMVAR model (Kalliovirta *et al.*, 2016, Virolainen, 2022).

We detrend the IPI by first separating its cyclical component from the trend with the linear projection filter proposed by Hamilton (2018) and then considering the cyclical component.⁶ It is thereby implicitly assumed that the monetary policy shock does not have permanent effects on real industrial production. Hereafter, we often refer to the IPI's deviation from the trend as the output gap. The logs of HCPI and the oil price are detrended by taking first differences, whereas the interest rate variable is assumed stationary. For numerical reasons, we multiply the cyclical component of the IPI and the log-difference of HCPI by 100, and the the log-difference of OIL by 10. The series are presented in Figure 1, where the shaded areas indicate the periods of Euro area recessions defined by the OECD.⁷

For selecting the order our G-StMVAR model, we started by estimating one-regime StMVAR models with autoregressive orders $p = 1, \dots, 12$ and found that AIC was minimized by the order $p = 1$. Then, we estimated a two-regime StMVAR model with $p = 1$ but found this model somewhat inadequate. Therefore, we increased the autoregressive order to $p = 2$, which increased the AIC. The overall adequacy of the StMVAR(2, 2) model, i.e., G-StMVAR($p = 2, M_1 = 0, M_2 = 2$) model, was found reasonable, so we employ it for the further analysis. Because the model does not contain large degrees of freedom parameter estimates, we do not consider incorporating Gaussian mixture components by switching to a G-StMVAR model with $M_1 > 0$. Details on model selection and the adequacy of the selected model are provided in Appendix C.1.

⁵ The IPI, HCPI, and EONIA were obtained from the European Central Bank Statistical Data Warehouse; the Brent crude oil prices were retrieved from the Federal Reserve Bank of St. Louis database; and the Wu and Xia (2016) shadow rate was obtained from the first author's website.

⁶ Denoting the univariate, non-stationary time series as y_t , the filter defines its transient component at the time $t + h$ ($h > 0$) as the ordinary least squares residuals from regressing y_{t+h} on a constant and y_t, \dots, y_{t-s+1} . When s is chosen larger than the order of integration, the residual process is stationary. We used the parameter values $h = 24$ and $s = 12$, as suggested by Hamilton (2018) for monthly data.

⁷ OECD Composite Leading Indicators, "Composite Leading Indicators: Reference Turning Points and Component Series", <http://www.oecd.org/std/leading-indicators/oecdcompositeleadingindicatorsreferenceturningpointsandcomponentseries.htm> (2.2.2022). At the time of accessing the series, the publicly available data ended at August 2021. We assume that the rest of the year 2021 did not contain recessions.

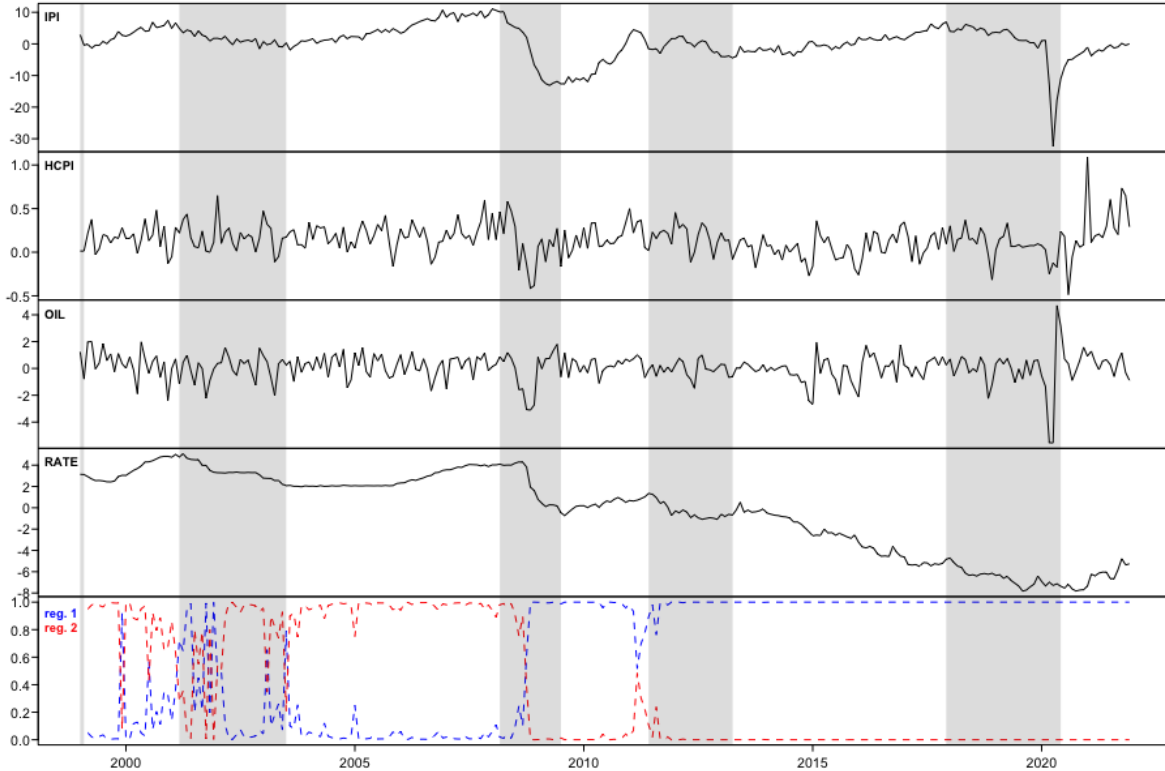


Figure 1: Monthly Euro area series covering the period from January 1999 to December 2021. The top panel presents the cyclical component of the industrial production index (IPI), which we separated from the trend using the linear projection filter proposed by Hamilton (2018). The second and third panels the log-differences of the harmonized consumer price index (HCPI) and Brent crude oil prices (Europe, OIL) multiplied by hundred and ten, respectively. The fourth panel presents an interest rate variable which is the EONIA from January 1999 to October 2008 and the Wu and Xia (2016) shadow rate from November 2008 to December 2021. The bottom panel shows the estimated mixing weights of the fitted StMVAR(2, 2) model. The shaded areas indicate the periods of Euro area recessions defined by the OECD.

The estimated mixing weights of the StMVAR(2, 2) model are presented in the bottom panel of Figure 1. The first regime (blue) mainly prevails after the Financial crisis in 2008, but it obtains large mixing weights also before and during the early 2000's recession. The second regime (red) dominates when the first one does not, that is, mainly before the Financial crisis. After the Financial crisis, its mixing weights stay close to zero, excluding a short period before the early 2010's recession, however. Since the prevailing regime starts switching sharply from the second to the first in October 2008, our model is consistent with the evidence that the ECB changed its reaction function after the bankruptcy of Lehman Brothers in September 2008 (Gerlach and Lewis, 2014).⁸

⁸ Gerlach and Lewis (2014) found that the ECB was cutting the interest rates faster at the time of the crisis, and that the ECB started a policy shift back in the late 2010. According our StMVAR model, however, the dominating regime never switches back to the pre-Financial crisis regime (in our sample period), although the second regime obtains mixing weights clearly larger than zero in the late 2010 and several relatively large mixing weights in the early 2011.

Based on unconditional means (and marginal variances) of the regimes (presented in Table 2 in Appendix C.2), the post-Financial crisis regime is characterized by negative (but volatile) output gap as well as lower inflation, oil price inflation, and interest rate variable than the pre-Financial crisis regime, which is characterized by positive output gap. The post-Financial crisis regime also exhibits higher kurtosis and overall volatility than the pre-Financial crisis regime. Details on the characteristics of the regimes are discussed in Appendix C.2. For the ease of communication, we will refer to the first regime as the low-growth post-Financial crisis regime and the second regime as the high-growth pre-Financial crisis regime without explicitly reminding that the classification is not a strict one: both regimes obtain large mixing weights before and after the Financial crisis, while both regimes also prevail during expansions and recessions.

7.1 Identification of a monetary policy shock

Decomposing the covariance matrices of the reduced form StMVAR(2, 2) model as in (4.5) gives the following estimates for the structural parameters:

$$\hat{W} = \begin{bmatrix} 0.77 (0.512) & -0.94 (0.618) & \mathbf{1.82} (0.771) & -0.13 (0.271) \\ -0.12 (0.069) & 0.12 (0.077) & \mathbf{0.17} (0.079) & 0.03 (0.026) \\ -\mathbf{1.05} (0.447) & -0.39 (0.482) & 0.56 (0.306) & 0.21 (0.143) \\ 0.01 (0.016) & -0.02 (0.022) & 0.02 (0.030) & \mathbf{0.50} (0.199) \end{bmatrix}, \quad \hat{\lambda}_2 = \begin{bmatrix} 0.50 (0.397) \\ 0.36 (0.291) \\ 0.19 (0.155) \\ 0.03 (0.021) \end{bmatrix}, \quad (7.1)$$

where the ordering of the variables is $y_t = (IPI_t, HCPI_t, OIL_t, RATE_t)$, the estimates $\hat{\lambda}_{2i}$ are in decreasing order (which fixes an arbitrary ordering for the columns of \hat{W}), and approximate standard errors are given in parentheses next to the estimates. The estimates that deviate from zero by more than two times their approximate standard error are bolded. We assume that the λ_{2i} are all distinct, i.e., Assumption 1.

The estimates and approximate standard errors in (7.1) show that the fourth shock is the only shock that moves the interest variable (also statistically) significantly at impact, while it is also the only shock that moves production to the opposite direction. Therefore, we deem it as the monetary policy shock. The fourth shock, however, appears to move inflation and oil price inflation to the same direction as the interest rate variable, which is contrary to many of the standard economic theories stating that an increase in the nominal interest rate should decrease inflation by decreasing aggregate demand (e.g., Galí, 2015, and the references therein).

The monetary policy shock is identified with Proposition 1 (Proposition 2 of Virolainen, 2022) by placing such constraints on W (or equivalently the B-matrix) that it is unambiguously distinguished from the other shocks. We assume that the monetary policy shock moves the interest rate and production in opposite directions and that it does not move inflation nor oil price inflation at impact. The zero constraints on inflation and oil price inflation obtained the p -values 0.22 and 0.15 in a Wald test individually and the p -value 0.34 jointly, so they are not rejected. These zero constraints are useful for distinguishing the monetary policy shock from the other shocks, but they also dampen the arguably implausible instantaneous increase in prices in response to a contractionary monetary

policy shock.⁹ The monetary policy shock is distinguished from the other shocks by assuming that first shock moves oil price inflation at impact and that the second and third shocks move inflation at impact. This is not economically restrictive, as the responses can be very small. The obtained estimates and their approximate standard errors are presented in Appendix C.3.¹⁰

7.2 Impulse response analysis

Following Virolainen (2022) (and others), we employ the generalized impulse response function (GIRF) (Koop, Pesaran, and Potter, 1996) for estimating the expected effects of the monetary policy shocks. The GIRF is defined as

$$\text{GIRF}(h, \delta_j, \mathcal{F}_{t-1}) = \text{E}[y_{t+h} | \delta_j, \mathcal{F}_{t-1}] - \text{E}[y_{t+h} | \mathcal{F}_{t-1}], \quad (7.2)$$

where $h \in \{0, 1, 2, \dots\}$ is the horizon and $\mathcal{F}_{t-1} = \sigma\{y_{t-j}, j > 0\}$ as before. The first term on the right side is the expected realization of the process at time $t + h$ conditionally on a structural shock of magnitude $\delta_j \in \mathbb{R}$ in the j th element of e_t at time t and the previous observations. The second term on the right side is the expected realization of the process conditionally on the previous observations only. The GIRF thus expresses the expected difference in the future outcomes when the structural shock of size δ_j in the j th element hits the system at time t as opposed to all shocks being random. It is interesting to also study the effects of the monetary policy shock to the mixing weights $\alpha_{m,t}$ in which case y_{t+h} is replaced with $\alpha_{m,t+h}$ on the right side of (7.2).

The G-StMVAR model has a p -step Markov property, so the GIRF can be calculated conditionally on the (σ -algebra generated by the) p previous observations $\mathbf{y}_{t-1} = (y_{t-1}, \dots, y_{t-p})$. We make use of this property by generating histories $\mathbf{y}_{t-1} = (y_{t-1}, \dots, y_{t-p})$ from the stationary distribution of each regime separately, and thereby obtain GIRFs conditional on the starting values being from this regime. The GIRFs and confidence intervals that reflect uncertainty about the initial value within the given regime are estimated using the Monte Carlo algorithm presented in Virolainen (2022), where the point estimate is the mean over the Monte Carlo replication and the confidence intervals are obtained from the empirical quantiles.

The StMVAR model accommodates asymmetries in the GIRFs with respect the initial state of the economy as well as to the sign and size of the shock. We study these three types of asymmetries by generating starting values from each regime separately and then estimating GIRFs for positive (contractionary) and negative (expansionary) one-standard-error (small) and two-standard-error (large) shocks. After estimating the GIRFs, we scale them so that they correspond to a 25 basis point instantaneous increase of the interest rate variable, making any asymmetries easy to detect.

⁹ Our results are, hence, contrary to Castelnuovo (2016) who argued that muted response of inflation in the Euro area could be caused by misspecified zero constraints in the impact matrix. Our model suggests that the zero constraints instead dampen the price puzzle (see Sims, 1992).

¹⁰The parameters λ_{2i} , $i = 1, \dots, 4$, were assumed distinct without a formal justification, which led to statistical identification of the model. However, by Proposition 3 of Virolainen (2022), the monetary policy shock is still identified if $\lambda_{2i} = \lambda_{2j}$ for any $i, j = 1, 2, 3$ and additionally $\lambda_{2i} = \lambda_{24}$ for any one of $i = 1, 2, 3$. But the approximate standard errors and the Wald test results are valid only if λ_{2i} are all distinct.

Figure 2 presents the GIRFs $h = 0, 1, \dots, 96$ months ahead estimated for the identified monetary policy shock.¹¹ The GIRFs of inflation and oil price inflation are accumulated to (scaled) log-levels. From top to bottom, the responses of IPI, HCPI, oil price, interest rate, and the first regime's mixing weights are depicted in each row, respectively. The first [third] column shows the responses to small contractionary (blue solid line) and expansionary (red dashed line) shocks with the initial values generated from the stationary distribution of the low-growth post-Financial crisis [high-growth pre-Financial crisis] regime. The second [fourth] column shows the responses to large contractionary and expansionary shocks with the initial values generated from the the low-growth post-Financial crisis [high-growth pre-Financial crisis] regime. The shaded areas are the 90% confidence intervals that reflect the uncertainty about the initial value within the given regime. Responses of the second regime's mixing weights are not depicted because they are the negative of those of the first regime.

In the low-growth post-Financial crisis regime (the first and second columns of Figure 2), the IPI decreases (increases) strongly at impact in response to a contractionary (expansionary) monetary policy shock. On average, the peak response is in the first period, and then the average response starts to slowly decay towards zero.¹² The confidence intervals show that with some of the starting values the peak effect occurs later, however. The effects seem to die out faster for an expansionary than a contractionary shock.

In response to a contractionary shock, the average price level stays roughly at zero for several years but decreases slowly and persistently. In response to an expansionary shock, the price level barely moves on average in the horizon of eight years, but confidence bounds show that with some of the starting values it decreases and from some increases.¹³ The oil price seems to increase (decrease) slightly for roughly fifteen months before it decreases (increases) persistently. The confidence bounds, however, show that with some starting values the expansionary shock may decrease the oil price. The interest rate variable stays high (low) very persistently, and the GIRFs seem quite symmetric with respect to the size of the shock.

In the high-growth pre-Financial crisis regime (the third and fourth columns of Figure 2), the IPI decreases (increases) strongly at impact as a response to a contractionary (expansionary) monetary policy shock. On average, the response then decreases (increases) and peaks roughly after two

¹¹We used $R_1 = R_2 = 2500$ in the Monte Carlo algorithm of Virolainen (2022). That is, for each regime as well as sign and size of the shock, we generated 2500 initial values, and for each of those initial values the GIRFs is estimated based on 2500 Monte Carlo repetitions.

¹²By zero, we mean the expected observation if all the shocks were random. Accordingly, by positive we mean expected observations larger than that and by negative expected observations smaller than that.

¹³The observation of prices rising in response to a contractionary monetary policy shock (or decreasing in response to an expansionary monetary policy shock) is often referred to as the price puzzle. Sims (1992) suggested that the price puzzle may appear if the monetary policy maker uses more information in predicting the future inflation than the autoregressive system of the variables included in the model. Consequently, the identified monetary policy shock would also contain a component that incorporates some of the policy maker's endogenous response to the prediction of the future inflation, which may then make it appear as if the prices increase (or decrease) in response to the shock. Another explanation proposes that the prices increase due to the cost-push effect of the monetary policy shock: an increase in the nominal interest rate increases the marginal cost of production of the firms who operate on borrowed money, and thereby decreases the aggregate supply and increases the price level (e.g., Barth and Ramey, 2001, Ravenna and Walsh, 2006). Several authors have, however, argued that the cost-channel is not likely strong enough to cause a price puzzle (e.g., Castelnuovo, 2012, Kaufmann and Scharler, 2009, Rabanal, 2007).

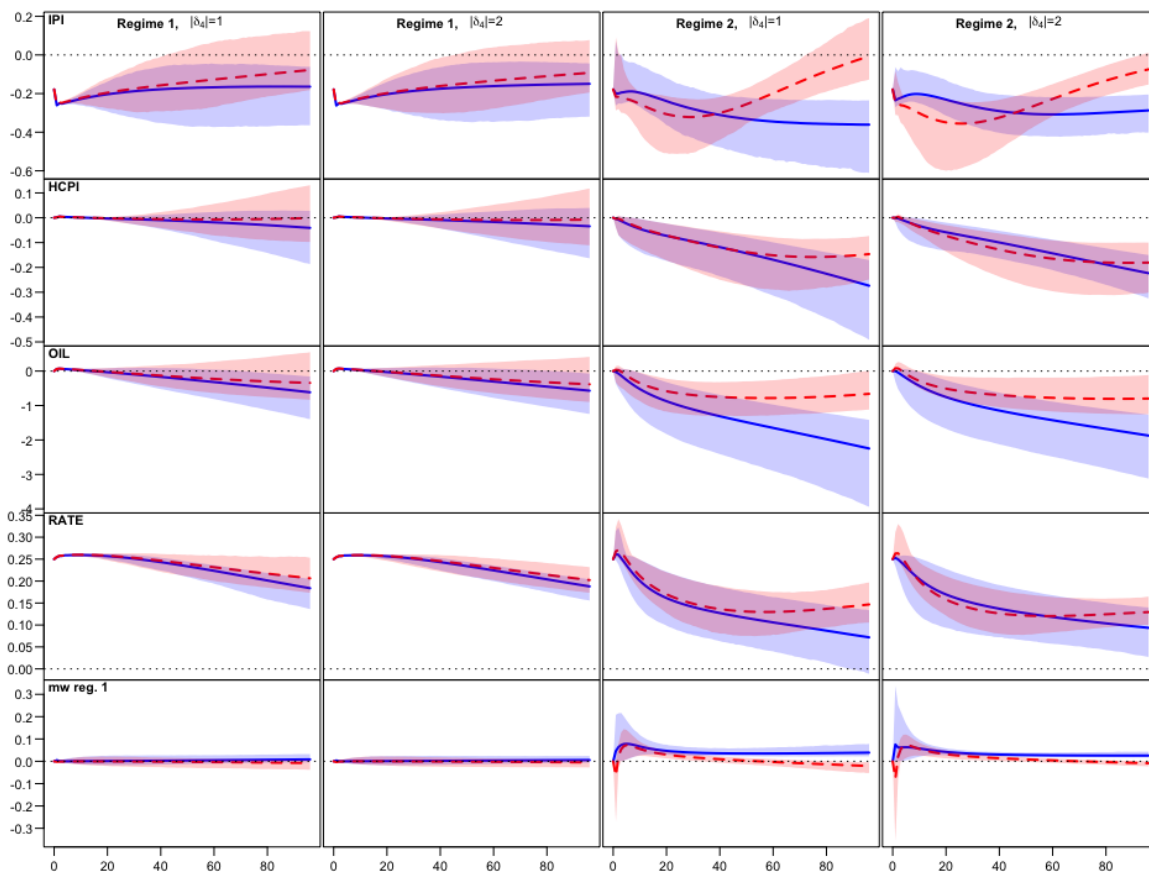


Figure 2: Generalized impulse response functions $h = 0, 1, \dots, 96$ months ahead estimated for the monetary policy shock identified in Section 7.1 using $R_1 = R_2 = 2500$ in the Monte Carlo algorithm presented in Virolainen (2022). From top to bottom, the responses of production, HCPI, oil price, the interest rate variable, and the first regime’s mixing weights are depicted in each row, respectively. The GIRFs of the HCPI and oil price are accumulated to (scaled) log-levels. The first [third] column shows the responses to one-standard-error contractionary (blue solid line) and expansionary (red dashed line) shocks with the initial values generated from the stationary distribution of the low-growth post-Financial crisis [high-growth pre-Financial crisis] regime. The second [fourth] column shows the responses to two-standard error contractionary and expansionary shocks with the initial values generated from the low-growth post-Financial crisis [high-growth pre-Financial crisis] regime. After estimation, all GIRFs were scaled so that the instantaneous movement of the interest rate variable is 25 basis points. The shaded areas are the 90% confidence intervals that reflect uncertainty about the initial state within the given regime. Responses of the second regime’s mixing weights are not depicted because they are the negative of those of the first regime.

and a half years for an expansionary shock, but stays low very persistently without a particular peak effect for a contractionary shock. The IPI stays low very persistently, because the probability of entering the low-growth post-Financial crisis regime stays above zero very persistently, as the responses of first regime's mixing weights show (the bottom panels of the third and fourth columns in Figure 2).

The price level starts to steadily decrease (increase) after the impact period. The average price level somewhat stabilizes roughly after two years when the shock is expansionary, but keeps decreasing over our horizon of eight years when the shock is contractionary. The confidence bounds show that with some of the initial values, the price level decays towards zero after several years when the shock is small and expansionary. The oil price moves similarly to the consumer prices, whereas the interest rate variable stays high (low) persistently, more so if the shock is expansionary. Interestingly, an expansionary shock significantly increases the probability of the low-growth regime in the first period, but in the following periods it significantly increases the probability of the high-growth regime.

Overall, we find strong asymmetries with respect to the initial state of the economy and the sign of the shock, but the asymmetries are weak with respect to the size of the shock. The real effects are less enduring for an expansionary shock than for a contractionary shock. Particularly in the high-growth regime, a contractionary shock persistently drives the economy towards the low-growth regime, which translates to very persistent decrease in the output gap. The inflationary effects of the monetary policy shock are stronger in the high-growth regime, while they are on average weak in the low-growth regime. In the low-growth regime, however, monetary policy is mainly measured with the Wu and Xia (2016) shadow rate instead of EONIA, which is mostly close to zero after the Financial crisis. Thus, the outcome might differ in the two regimes also due to the different measures of monetary policy.

8 Summary

We introduced a new mixture vector autoregressive model, which has attractive theoretical and practical properties. The G-StMVAR model accommodates conditionally homoskedastic Gaussian VARs and conditionally heteroskedastic Student's t VARs as its mixture components. The mixing weights are defined as weighted ratios of the component process stationary densities corresponding to p previous observations. Therefore, the greater the relative weighted likelihood of a regime is, the more likely the process is to generate an observation from it. This facilitates associating statistical characteristic and economic interpretations to the regimes. The specific formulation of the mixing weights also leads to attractive theoretical properties such as ergodicity and full knowledge of the stationary distribution of $p+1$ consecutive observations. Moreover, the maximum likelihood estimator of a stationary G-StMVAR model is strongly consistent, and therefore, it has the conventional limiting distribution under conventional high level conditions.

The G-StMVAR model is a multivariate version of the G-StMAR model of Virolainen (forthcoming). As special case, by assuming that all the mixture components are linear Student's t VARs, we also obtained a multivariate version of the StMAR model of Meitz *et al.* (forthcoming), which we

call the StMVAR model. In addition to the reduced form model, we introduced a structural version of the G-StMVAR model with a time-varying impact matrix and statistically identified shocks. Referring to Virolainen (2022), we discussed the problem of identifying the structural shocks and presented a general set of conditions for identifying any subset of the shocks. We then employed the structural model in the empirical application. The accompanying CRAN distributed R package `gmvar` (Virolainen, 2018a) provides a comprehensive set of tools for maximum likelihood estimation and other numerical analysis of the introduced models.

The empirical application studied asymmetries in the expected effects of the monetary policy shock in the Euro area and considered a monthly data covering the period from January 1999 to December 2021. Our StMVAR model identified two regimes: a low-growth regime and a high-growth regime. The low-growth regime is characterized by a negative (but volatile) output gap, and it mainly prevails after the collapse of Lehman Brothers in the Financial crisis but obtains large mixing weights also during and before the early 2000's recession. The high-growth regime is characterized by a positive output gap and it mainly dominates before the Financial crisis.

We found strong asymmetries with respect to the initial state of the economy and the sign of the shock, but asymmetries with respect to the size of the shock were weak. The real effects are less enduring for an expansionary shock than for a contractionary shock. Particularly in the high-growth pre-Financial crisis regime, a contractionary shock persistently drives the economy towards the low-growth post-Financial crisis regime, which translates to a very persistent decrease in the output gap. The inflationary effects of the monetary policy shock are stronger in the high-growth regime than in the low-growth regime, and in the latter the price level did not move much on average. In the low-growth regime, however, monetary policy is mainly measured with the Wu and Xia (2016) shadow rate instead of EONIA, which is mostly close to zero after the Financial crisis.

References

- Barth M. J., Ramey V. A. (2001). "The Cost Channel of Monetary Transmission." In BS Bernanke, K Rogoff (eds.), *NBER Macroeconomics Annual*, volume 16, pp. 199–239. MIT Press, Cambridge.
- Burgard J., Neuenkirch M., Nöckel M. (2019). "State-Dependent Transmission of Monetary Policy in the Euro Area." *Journal of Money, Credit and Banking*, **51**(7), 2053–2070.
- Castelnuovo E. (2012). "Testing the Structural Interpretation of the Price Puzzle with a Cost-Channel Model." *Oxford Bulletin of Economics and Statistics*, **74**(3), 425–452.
- Castelnuovo E. (2016). "Monetary policy shocks and Cholesky VARs: an assessment for the Euro area." *Empirical Economics*, **50**, 383–414.
- Ding P. (2016). "On the Conditional Distribution of the Multivariate t Distribution." *The American Statistician*, **70**(3), 293–295.
- Dolado J. J., María-Dolores R. (2006). "State Asymmetries in the Effects of Monetary Policy Shocks on Output: Some New Evidence for the Euro-Area." In C Milas, P Rothman, D van Dijk (eds.), *Nonlinear Time Series Analysis of Business Cycles*, pp. 311–331. Emerald Publishing Limited.

- Galí J. (2015). *Monetary Policy, Inflation, and the Business Cycle*. 2nd edition. Princeton University Press, Princeton and Oxford.
- Gerlach S., Lewis J. (2014). “ECB Reaction Functions and the Crisis of 2008.” *International Journal of Central Banking*, **10**(1), 137–158.
- Hamilton J. D. (2018). “WHY YOU SHOULD NEVER USE THE HODRICK-PRESCOTT FILTER.” *The Review of Economics and Statistics*, **100**(5), 831–843.
- Heracleous M. S. (2003). *Volatility Modeling Using the Student’s t Distribution*. Ph.D. thesis, Virginia Tech.
- Holzmann H., Munk A., Gneiting T. (2006). “Identifiability of finite mixtures of elliptical distributions.” *Scandinavian Journal of Statistics*, **33**(4), 753–763.
- Kalliovirta L. (2012). “Misspecification tests based on quantile residuals.” *The Econometrics Journal*, **15**(2), 358–393.
- Kalliovirta L., Meitz M., Saikkonen P. (2015). “A Gaussian Mixture Autoregressive Model for Univariate Time Series.” *Journal of Time Series Analysis*, **36**(2), 247–266.
- Kalliovirta L., Meitz M., Saikkonen P. (2016). “Gaussian mixture vector autoregression.” *Journal of Econometrics*, **192**(2), 465–498.
- Kalliovirta L., Saikkonen P. (2010). “Reliable Residuals for Multivariate Nonlinear Time Series Models.” *Unpublished revision of HECER discussion paper No. 247*.
- Kaufmann S., Scharler J. (2009). “Financial systems and the cost channel transmission of monetary policy shocks.” *Economic Modelling*, **26**(1), 40–46.
- Koop G., Pesaran M., Potter S. (1996). “Impulse response analysis in nonlinear multivariate models.” *Journal of Econometrics*, **74**(1), 119–147.
- Lanne M., Lütkepohl H. (2010). “Structural Vector Autoregressions With Nonnormal Residuals.” *Journal of Business & Economic Statistics*, **28**(1), 159–168.
- Lanne M., Lütkepohl H., Maciejowska K. (2010). “Structural vector autoregressions with Markov switching.” *Journal of Economic Dynamics and Control*, **34**(2), 121–131.
- Lütkepohl H. (2005). *New Introduction to Multiple Time Series Analysis*. 1st edition. Springer, Berlin.
- Meitz M., Preve D., Saikkonen P. (2018). *StMAR Toolbox: A MATLAB Toolbox for Student’s t Mixture Autoregressive Models*.
- Meitz M., Preve D., Saikkonen P. (forthcoming). “A mixture autoregressive model based on Student’s t -distribution.” *Communications in Statistics - Theory and Methods*.
- Meitz M., Saikkonen P. (2021). “Testing for observation-dependent regime switching in mixture autoregressive models.” *Journal of Econometrics*, **222**(1), 601–624.
- Meyn S., Tweedie R. (2009). *Markov Chains and Stochastic Stability*. 2nd edition. Cambridge University Press, Cambridge.
- Muirhead R. (1982). *Aspects of Multivariate Statistical Theory*. 1st edition. John Wiley & Sons, Hoboken, New Jersey.

- Newey W., McFadden D. (1994). “Large sample estimation and hypothesis testing.” In R. Engle, D. MacFadden (eds.), *Handbook of Econometrics*, volume 4, chapter 36. Elsevier Science B.V.
- Peersman G., Smets F. (2002). “Are the effects of monetary policy in the euro area greater in recessions than in booms?” In L. Mahadeva, P. Sinclair (eds.), *Monetary Transmission in Diverse Economies*, pp. 28–48. Cambridge University Press.
- Pellegrino G. (2018). “Uncertainty and the real effects of monetary policy shocks in the Euro area.” *Economics Letters*, **162**, 177–181.
- Poudyal N. (2012). *Confronting Theory with Data: the Case of DSGE Modeling*. Ph.D. thesis, Virginia Tech.
- Rabanal P. (2007). “Does inflation increase after a monetary policy tightening? Answers based on an estimated DSGE model.” *Journal of Economic Dynamics and Control*, **31**(3), 906–937.
- Ranga Rao R. (1962). “Relations between Weak and Uniform Convergence of Measures with Applications.” *The Annals of Mathematical Statistics*, **33**(2), 659–680.
- Ravenna F., Walsh C. (2006). “Optimal monetary policy with the cost channel.” *Journal of Monetary Economics*, **53**(2), 199–216.
- Redner R., Walker H. (1984). “Mixture Densities, Maximum Likelihood and the Em Algorithm.” *Society for Industrial and Applied Mathematics*, **26**(2), 195–239.
- Sims A. (1992). “Interpreting the macroeconomic time series facts.” *European economic review*, **36**(5), 975–1000.
- Virolainen S. (2018a). *gmvarKit: Estimate Gaussian and Student’s t Mixture Vector Autoregressive Models*. R package version 2.0.3 available at CRAN: <https://CRAN.R-project.org/package=gmvarKit>.
- Virolainen S. (2018b). *uGMAR: Estimate Univariate Gaussian and Student’s t Mixture Autoregressive Models*. R package version 3.4.2 available at CRAN: <https://CRAN.R-project.org/package=uGMAR>.
- Virolainen S. (2022). “Structural Gaussian Mixture vector autoregressive model with application to the asymmetric effects of monetary policy shocks.” *Unpublished working paper, available as arXiv:2007.04713*.
- Virolainen S. (forthcoming). “A mixture autoregressive model based on Gaussian and Student’s *t*-distributions.” *Studies in Nonlinear Dynamics & Econometrics*.
- Wu J., Xia F. (2016). “Measuring the Macroeconomic Impact of Monetary Policy at the Zero Lower Bound.” *Journal of Money, Credit and Banking*, **48**(2-3), 253–291.

Appendix A Properties of multivariate Gaussian and Student's t distribution

Denote a d -dimensional real valued vector by y . It is well known that the density function of a d -dimensional Gaussian distribution with mean μ and covariance matrix Σ is

$$n_d(y; \mu, \Sigma) = (2\pi)^{-d/2} \det(\Sigma)^{-1/2} \exp \left\{ -\frac{1}{2} (y - \mu)' \Sigma^{-1} (y - \mu) \right\}. \quad (\text{A.1})$$

Similarly to Meitz *et al.* (forthcoming) but differing from the standard form, we parametrize the Student's t -distribution using its covariance matrix as a parameter together with the mean and the degrees of freedom. The density function of such a d -dimensional t -distribution with mean μ , covariance matrix Σ , and $\nu > 2$ degrees of freedom is (see, e.g., Appendix A in Meitz *et al.*, forthcoming)

$$t_d(y; \mu, \Sigma, \nu) = C_d(\nu) \det(\Sigma)^{-1/2} \left(1 + \frac{(y - \mu)' \Sigma^{-1} (y - \mu)}{\nu - 2} \right)^{-(d+\nu)/2}, \quad (\text{A.2})$$

where

$$C_d(\nu) = \frac{\Gamma\left(\frac{d+\nu}{2}\right)}{\sqrt{\pi^d (\nu - 2)^d} \Gamma\left(\frac{\nu}{2}\right)}, \quad (\text{A.3})$$

and $\Gamma(\cdot)$ is the gamma function. We assume that the covariance matrix Σ is positive definite for both distributions.

Consider a partition $X = (X_1, X_2)$ of either Gaussian or t -distributed (with ν degrees of freedom) random vector X such that X_1 has dimension $(d_1 \times 1)$ and X_2 has dimension $(d_2 \times 1)$. Consider also a corresponding partition of the mean vector $\mu = (\mu_1, \mu_2)$ and the covariance matrix

$$\Sigma = \begin{bmatrix} \Sigma_{11} & \Sigma_{12} \\ \Sigma'_{12} & \Sigma_{22} \end{bmatrix}, \quad (\text{A.4})$$

where, for example, the dimension of Σ_{11} is $(d_1 \times d_1)$. In the Gaussian case, X_1 then has the marginal distribution $n_{d_1}(\mu_1, \Sigma_{11})$ and X_2 has the marginal distribution $n_{d_2}(\mu_2, \Sigma_{22})$. In the Student's t case, X_1 has the marginal distribution $t_{d_1}(\mu_1, \Sigma_{11}, \nu)$ and X_2 has the marginal distribution $t_{d_2}(\mu_2, \Sigma_{22}, \nu)$ (see, e.g., Ding (2016), also in what follows).

When X has Gaussian distribution, the conditional distribution of the random vector X_1 given $X_2 = x_2$ is

$$X_1 \mid (X_2 = x_2) \sim n_{d_1}(\mu_{1|2}(x_2), \Sigma_{1|2}(x_2)), \quad (\text{A.5})$$

where

$$\mu(x_2) \equiv \mu_{1|2}(x_2) = \mu_1 + \Sigma_{12} \Sigma_{22}^{-1} (x_2 - \mu_2) \quad \text{and} \quad (\text{A.6})$$

$$\Omega \equiv \Sigma_{1|2}(x_2) = \Sigma_{11} - \Sigma_{12} \Sigma_{22}^{-1} \Sigma'_{12}. \quad (\text{A.7})$$

When X has t -distribution, the conditional distribution of the random vector X_1 given $X_2 = x_2$ is

$$X_1 \mid (X_2 = x_2) \sim t_{d_1}(\mu_{1|2}(x_2), \Sigma_{1|2}(x_2), \nu + d_2), \quad (\text{A.8})$$

where

$$\mu(x_2) = \mu_{1|2}(x_2) = \mu_1 + \Sigma_{12}\Sigma_{22}^{-1}(x_2 - \mu_2) \quad \text{and} \quad (\text{A.9})$$

$$\Omega(x_2) \equiv \Sigma_{1|2}(x_2) = \frac{\nu - 2 + (x_2 - \mu_2)'\Sigma_{22}^{-1}(x_2 - \mu_2)}{\nu - 2 + d_2}(\Sigma_{11} - \Sigma_{12}\Sigma_{22}^{-1}\Sigma_{12}'). \quad (\text{A.10})$$

In particular, we have

$$n_d(x; \mu, \Sigma) = n_{d_1}(x_1; \mu_{1|2}(x_2), \Sigma_{1|2}(x_2))n_{d_2}(x_2; \mu_2, \Sigma_{22}) \quad \text{and} \quad (\text{A.11})$$

$$t_d(x; \mu, \Sigma, \nu) = t_{d_1}(x_1; \mu_{1|2}(x_2), \Sigma_{1|2}(x_2), \nu + d_2)t_{d_2}(x_2; \mu_2, \Sigma_{22}, \nu). \quad (\text{A.12})$$

Appendix B Proofs

B.1 Proof of Theorem 1

Corresponding to $\phi_0 \in \mathbb{R}^d$, $\mathbf{A}_p \in \mathbb{S}^{d \times dp}$, $\Omega \in \mathbb{R}^{d \times d}$ positive definite, and $\nu > 2$, define the notation μ , Σ_p , $\Sigma_1(h)$ ($h = 0, 1, \dots, p$), Σ_{1p} , and Σ_{p+1} as in (2.4)-(2.6). Note that by construction and the assumption $\mathbf{A}_p \in \mathbb{S}^{d \times dp}$, Σ_p and Σ_{p+1} are symmetric positive definite block Toeplitz matrices with the $(d \times d)$ blocks $\Sigma_1(h)$, $h = 0, 1, \dots, p$. Analogously to Meitz *et al.* (forthcoming), we prove Part (i) by constructing a dp -dimensional Markov chain $\mathbf{z}_t = (z_t, \dots, z_{t-p+1})$ ($t = 1, 2, \dots$) with the desired properties. Then, we make use of the theory of Markov chains to establish its stationary distribution. To that end, an appropriate transition probability measure and an initial distribution needs to be specified. For the former, assume that the transition probability of \mathbf{z}_t is determined by the density function $t_d(z_t; \mu(\mathbf{z}_{t-1}), \Omega(\mathbf{z}_{t-1}), \nu + dp)$, where $\mu(\mathbf{z}_{t-1})$ and $\Omega(\mathbf{z}_{t-1})$ are obtained from (A.9) and (A.10), respectively, by replacing x_2 with \mathbf{z}_{t-1} . Because the distribution of the current observation depends only on the previous one, \mathbf{z}_t is a Markov chain on \mathbb{R}^{dp} .

Suppose the initial value \mathbf{z}_0 follows the t -distribution $t_{dp}(\mathbf{1}_p \otimes \mu, \Sigma_p, \nu)$. The properties of t -distribution (given in Appendix A) then imply that if $\mathbf{z}_t^+ = (z_t, \mathbf{z}_{t-1})$, the density function of \mathbf{z}_1^+ is given by

$$t_{d(p+1)}(\mathbf{z}_1^+; \mathbf{1}_{p+1} \otimes \mu, \Sigma_{p+1}, \nu) = t_d(z_1; \mu(\mathbf{z}_0), \Omega(\mathbf{z}_0), \nu + dp)t_{dp}(\mathbf{z}_0; \mathbf{1}_p \otimes \mu, \Sigma_p, \nu). \quad (\text{B.1})$$

Thus, $\mathbf{z}_1^+ \sim t_{d(p+1)}(\mathbf{1}_{p+1} \otimes \mu, \Sigma_{p+1}, \nu)$, and from the block Toeplitz structure of Σ_{p+1} it follows that the marginal distribution of \mathbf{z}_1 is the same as that of \mathbf{z}_0 , i.e., $\mathbf{z}_1 \sim t_{dp}(\mathbf{1}_p \otimes \mu, \Sigma_p, \nu)$. Hence, as \mathbf{z}_t is a Markov chain, it has a stationary distribution characterized by the density $t_{dp}(\mathbf{1}_p \otimes \mu, \Sigma_p, \nu)$ (Meyn and Tweedie, 2009, pp. 230-231), completing the proof of Part (i).

Denote by \mathcal{F}_{t-1}^z the σ -algebra generated by the random variables $\{z_s, s < t\}$. To prove Part (ii), note that due to the Markov property, $z_t | \mathcal{F}_{t-1}^z \sim t_d(\mu(\mathbf{z}_0), \Omega(\mathbf{z}_0), \nu + dp)$. Therefore, the conditional expectation and conditional variance of z_t given \mathcal{F}_{t-1}^z can be written as

$$E[z_t | \mathcal{F}_{t-1}^z] = E[z_t | \mathbf{z}_{t-1}] = \mu + \Sigma_{1p}\Sigma_p^{-1}(\mathbf{z}_{t-1} - \mathbf{1}_p \otimes \mu) = \phi_0 + \mathbf{A}_p \mathbf{z}_{t-1}, \quad (\text{B.2})$$

$$\text{Var}[z_t | \mathcal{F}_{t-1}^z] = \text{Var}[z_t | \mathbf{z}_{t-1}] = \frac{\nu - 2 + (\mathbf{z}_{t-1} - \mathbf{1}_p \otimes \mu)'\Sigma_p^{-1}(\mathbf{z}_{t-1} - \mathbf{1}_p \otimes \mu)}{\nu - 2 + dp}\Omega, \quad (\text{B.3})$$

where $\Omega = \Sigma_1 - \Sigma_{1p}\Sigma_p^{-1}\Sigma'_{1p}$. We denote this conditional variance by $\Omega_t \equiv \Omega(\mathbf{z}_{t-1})$, which is positive definite due to the assumptions $\nu > 2$ and that Σ_p and Ω are both positive definite. Define the $(d \times 1)$ random vectors ε_t as

$$\varepsilon_t \equiv \Omega_t^{-1/2}(z_t - \phi_0 - \mathbf{A}_p \mathbf{z}_{t-1}), \quad (\text{B.4})$$

where $\Omega_t^{-1/2}$ is a symmetric square root matrix of Ω_t^{-1} . Conditionally on \mathcal{F}_{t-1}^z , ε_t now follow the $t_d(0, I_d, \nu + dp)$ distribution, and therefore the 'VAR(p)-ARCH(p)' representation (2.10) is obtained. Because this conditional distribution does not depend on \mathcal{F}_{t-1}^z , it follows that the unconditional distribution of ε_t is also $t_d(0, I_d, \nu + dp)$. Hence, ε_t is independent of \mathcal{F}_{t-1}^z (or of $\{z_s, s < t\}$), and as the random vectors $\{\varepsilon_s, s < t\}$ are functions of $\{z_s, s < t\}$, ε_t is also independent of $\{\varepsilon_s, s < t\}$. Thus, the proof of Part (ii) is completed by concluding that the random vectors ε_t are IID $t_d(0, I_d, \nu + dp)$ distributed. ■

B.2 Proof of Theorem 2

The G-StMVAR process \mathbf{y}_t is clearly a Markov chain on \mathbb{R}^{dp} . Let $\mathbf{y}_0 = (y_0, \dots, y_{-p+1})$ be random vector whose distribution is characterized by the density $f(\mathbf{y}_0; \boldsymbol{\theta}) = \sum_{m=1}^{M_1} \alpha_m n_{dp}(\mathbf{y}_0; \mathbf{1}_p \otimes \mu_m, \Sigma_{m,p}) + \sum_{m=M_1+1}^M \alpha_m t_{dp}(\mathbf{y}_0; \mathbf{1}_p \otimes \mu_m, \Sigma_{m,p}, \nu_m)$. According to (2.3), (3.1), (3.5), and (B.1), the conditional density of y_1 given \mathbf{y}_0 is

$$\begin{aligned} f(y_1 | \mathbf{y}_0; \boldsymbol{\theta}) &= \sum_{m=1}^{M_1} \frac{\alpha_m n_{dp}(\mathbf{y}_0; \mathbf{1}_p \otimes \mu_m, \Sigma_{m,p})}{f(\mathbf{y}_0; \boldsymbol{\theta})} n_d(y_1; \mu_{m,1}(\mathbf{y}_0), \Omega_{m,1}) \\ &\quad + \sum_{m=M_1+1}^M \frac{\alpha_m t_{dp}(\mathbf{y}_0; \mathbf{1}_p \otimes \mu_m, \Sigma_{m,p}, \nu_m)}{f(\mathbf{y}_0; \boldsymbol{\theta})} t_d(y_1; \mu_{m,1}(\mathbf{y}_0), \Omega_{m,1}(\mathbf{y}_0), \nu_m + dp) \end{aligned} \quad (\text{B.5})$$

$$\begin{aligned} &= \sum_{m=1}^{M_1} \frac{\alpha_m}{f(\mathbf{y}_0; \boldsymbol{\theta})} n_{d(p+1)}((y_1, \mathbf{y}_0); \mathbf{1}_{p+1} \otimes \mu_m, \Sigma_{m,p+1}) \\ &\quad + \sum_{m=M_1+1}^M \frac{\alpha_m}{f(\mathbf{y}_0; \boldsymbol{\theta})} t_{d(p+1)}((y_1, \mathbf{y}_0); \mathbf{1}_{p+1} \otimes \mu_m, \Sigma_{m,p+1}, \nu_m). \end{aligned} \quad (\text{B.6})$$

The random vector (y_1, \mathbf{y}_0) therefore has the density

$$\begin{aligned} f(y_1, \mathbf{y}_0) &= \sum_{m=1}^{M_1} \alpha_m n_{d(p+1)}((y_1, \mathbf{y}_0); \mathbf{1}_{p+1} \otimes \mu_m; \Sigma_{m,p+1}) \\ &\quad + \sum_{m=M_1+1}^M \alpha_m t_{d(p+1)}((y_1, \mathbf{y}_0); \mathbf{1}_{p+1} \otimes \mu_m; \Sigma_{m,p+1}, \nu_m). \end{aligned} \quad (\text{B.7})$$

Integrating y_{-p+1} out, and using the properties of marginal distributions of a multivariate Gaussian and t -distributions (see Appendix A) together with the block Toeplitz form of $\Sigma_{m,p+1}$ shows that

the density of \mathbf{y}_1 is $f(\mathbf{y}_1; \boldsymbol{\theta}) = \sum_{m=1}^{M_1} \alpha_m n_{dp}(\mathbf{y}_1; \mathbf{1}_p \otimes \mu_m, \Sigma_{m,p}) + \sum_{m=M_1+1}^M \alpha_m t_{dp}(\mathbf{y}_1; \mathbf{1}_p \otimes \mu_m, \Sigma_{m,p}, \nu_m)$. Thus, \mathbf{y}_0 and \mathbf{y}_1 are identically distributed. As $\{\mathbf{y}_t\}_{t=1}^\infty$ is a (time-homogeneous) Markov chain, it follows that $\{\mathbf{y}_t\}_{t=1}^\infty$ has a stationary distribution, say $\pi_{\mathbf{y}}(\cdot)$, characterized by the density $f(\cdot; \boldsymbol{\theta}) = \sum_{m=1}^{M_1} \alpha_m n_{dp}(\cdot; \mathbf{1}_p \otimes \mu_m, \Sigma_{m,p}) + \sum_{m=M_1+1}^M \alpha_m t_{dp}(\cdot; \mathbf{1}_p \otimes \mu_m, \Sigma_{m,p}, \nu_m)$ (Meyn and Tweedie, 2009, pp. 230-231).

For ergodicity, let $P_{\mathbf{y}}(\mathbf{y}, \cdot) = \mathbb{P}(\mathbf{y}_p \in \cdot | \mathbf{y}_0 = \mathbf{y})$ signify the p -step transition probability measure of the process \mathbf{y}_t . Using the p th order Markov property of y_t , it is straightforward to check that $P_{\mathbf{y}}(\mathbf{y}, \cdot)$ has the density

$$f(\mathbf{y}_p | \mathbf{y}_0; \boldsymbol{\theta}) = \prod_{t=1}^p f(y_t | \mathbf{y}_{t-1}; \boldsymbol{\theta}) = \prod_{t=1}^p \left(\sum_{m=1}^{M_1} \alpha_m n_d(y_t; \mu_{m,t}(\mathbf{y}_{t-1}), \Omega_m) + \sum_{m=M_1+1}^M \alpha_m t_d(y_t; \mu_{m,t}(\mathbf{y}_{t-1}), \Omega_{m,t}(\mathbf{y}_{t-1}), \nu_m + dp) \right). \quad (\text{B.8})$$

Clearly, $f(\mathbf{y}_p | \mathbf{y}_0; \boldsymbol{\theta}) > 0$ for all $\mathbf{y}_0 \in \mathbb{R}^{dp}$ and $\mathbf{y}_p \in \mathbb{R}^{dp}$, so it can be concluded that \mathbf{y}_t is ergodic in the sense of (Meyn and Tweedie, 2009, Chapter 13) by using arguments identical to those used in the proof of Theorem 1 in Kalliovirta *et al.* (2015). ■

B.3 Proof of Theorem 3

First note that $L_T^{(c)}(\boldsymbol{\theta})$ is continuous and that together with Assumption 2 it implies existence of a measurable maximizer $\hat{\boldsymbol{\theta}}_T$. To conclude that $\hat{\boldsymbol{\theta}}_T$ is strongly consistent, we need to show that (see, e.g., Newey and McFadden, 1994, Theorem 2.1 and the discussion on page 2122)

- (i) the uniform strong law of large numbers holds for the log-likelihood function; that is,

$$\sup_{\boldsymbol{\theta} \in \Theta} \left| L_T^{(c)}(\boldsymbol{\theta}) - E[L_T^{(c)}(\boldsymbol{\theta})] \right| \rightarrow 0 \quad \text{almost surely as } T \rightarrow \infty,$$

- (ii) and that the limit of $L_T^{(c)}(\boldsymbol{\theta})$ is uniquely maximized at $\boldsymbol{\theta} = \boldsymbol{\theta}_0$.

Proof of (i). By Theorem 2, the process $\mathbf{y}_{t-1} = (y_t, \dots, y_{t-p+1})$, and hence also y_t , is stationary and ergodic, and $E[L_T^{(c)}(\boldsymbol{\theta})] = E[l_t(\boldsymbol{\theta})]$. To conclude (i), it therefore suffices to show that $E[\sup_{\boldsymbol{\theta} \in \Theta} |l_t(\boldsymbol{\theta})|] < \infty$ (see Ranga Rao, 1962). We will do that by making use of the compactness of the parameter space to derive finite lower and upper bounds for $l_t(\boldsymbol{\theta})$, which is given as

$$l_t(\boldsymbol{\theta}) = \log \left(\sum_{m=1}^{M_1} \alpha_{m,t} n_d(y_t; \mu_{m,t}, \Omega_m) + \sum_{m=M_1+1}^M \alpha_{m,t} t_d(y_t; \mu_{m,t}, \Omega_{m,t}, \nu_m + dp) \right). \quad (\text{B.9})$$

First, we derive an upper bound for the normal distribution densities. Determinant of the positive definite conditional covariance matrix Ω_m is a continuous function of the parameters $\text{vech}(\Omega_m)$,

and hence, compactness of the parameter space implies that the determinant is bounded from below by some constant that is strictly larger than zero and from above by some finite constant. Thus,

$$0 < c_1 \leq \det(\Omega_m)^{-1/2} \leq c_2 < \infty, \quad (\text{B.10})$$

for some constants c_1 and c_2 . Because Ω_m^{-1} is positive definite and exponential function is bounded from above by one in the non-positive real axis, we obtain the upper bound

$$n_d(y_t; \mu_{m,t}, \Omega_m) = (2\pi)^{-d/2} \det(\Omega_m)^{-1/2} \exp \left\{ -\frac{1}{2} (y_t - \mu_m)' \Omega_m^{-1} (y_t - \mu_m) \right\} \leq (2\pi)^{-d/2} c_2. \quad (\text{B.11})$$

Next, we derive an upper bound for the t -distribution densities

$$\begin{aligned} t_d(y_t; \mu_{m,t}, \Omega_{m,t}, \nu_m + dp) &= \frac{\Gamma \left(\frac{\nu_m + (1+p)d}{2} \right)}{\sqrt{\pi^d (\nu_m + dp - 2)^d} \Gamma \left(\frac{\nu_m + dp}{2} \right)} \det(\Omega_{m,t})^{-1/2} \\ &\times \left(1 + \frac{(y_t - \mu_{m,t})' \Omega_{m,t}^{-1} (y_t - \mu_{m,t})}{\nu_m + dp - 2} \right)^{-(\nu_m + d(1+p))/2}. \end{aligned} \quad (\text{B.12})$$

Since $\nu_m > 2$ and the parameter space is compact, $2 < c_3 \leq \nu_m \leq c_4 < \infty$ for some constants c_3 and c_4 . Because the gamma function is continuous on the positive real axis, it then follows that

$$0 < c_5 \leq \frac{\Gamma \left(\frac{\nu_m + (1+p)d}{2} \right)}{\sqrt{\pi^d (\nu_m + dp - 2)^d} \Gamma \left(\frac{\nu_m + dp}{2} \right)} \leq c_6 \quad (\text{B.13})$$

for some finite constants c_5 and c_6 .

Using the bounds $2 < c_3 \leq \nu_m \leq c_4 < \infty$ and (B.10) together with the fact that $\Sigma_{m,p}^{-1}$ is positive definite gives

$$\begin{aligned} \det(\Omega_{m,t})^{-1/2} &= \left(\frac{\nu_m - 2 + (\mathbf{y}_{t-1} - \mathbf{1}_p \otimes \mu_m)' \Sigma_{m,p}^{-1} (\mathbf{y}_{t-1} - \mathbf{1}_p \otimes \mu_m)}{\nu_m - 2 + dp} \right)^{-d/2} \det(\Omega_m)^{-1/2} \\ &\leq \left(\frac{c_3 - 2}{c_4 + dp - 2} \right)^{-d/2} c_2 < \infty. \end{aligned} \quad (\text{B.14})$$

For a lower bound, note that $\Sigma_{m,p}^{-1}$ is a continuous function of the parameters and thereby its eigenvalues are as well. It then follows from the compactness of the parameter space that its largest eigenvalue, λ_1^{max} , is bounded from above by some finite constant, say c_7 . The compactness of the parameter space also implies that there exist finite constant c_8 such that $\mu_{im} \leq c_8$ for all $i = 1, \dots, d$ (where μ_{im} is the i th element of μ_m). By using the orthonormal spectral decomposition of $\Sigma_{m,p}^{-1}$, we then obtain

$$\begin{aligned} (\mathbf{y}_{t-1} - \mathbf{1}_p \otimes \mu_m)' \Sigma_{m,p}^{-1} (\mathbf{y}_{t-1} - \mathbf{1}_p \otimes \mu_m) &\leq \lambda_1^{max} (\mathbf{y}_{t-1} - \mathbf{1}_p \otimes \mu_m)' (\mathbf{y}_{t-1} - \mathbf{1}_p \otimes \mu_m) \\ &\leq c_7 (\mathbf{y}'_{t-1} \mathbf{y}_{t-1} - 2c_8 \mathbf{y}'_{t-1} \mathbf{1}_{dp} + dpc_8^2). \end{aligned} \quad (\text{B.15})$$

Thus,

$$\det(\Omega_{m,t})^{-1/2} \geq \left(\frac{c_4 - 2 + c_7(\mathbf{y}'_{t-1}\mathbf{y}_{t-1} - 2c_8\mathbf{y}'_{t-1}\mathbf{1}_{dp} + dpc_8^2)}{c_3 - 2 + dp} \right)^{-d/2} c_1. \quad (\text{B.16})$$

As $-(\nu_m + (1+p)d)/2 < 0$ and $\Omega_{m,t}^{-1}$ is positive definite, we have that

$$\left(1 + \frac{(\mathbf{y}_t - \mu_{m,t})'\Omega_{m,t}^{-1}(\mathbf{y}_t - \mu_{m,t})}{\nu_m + dp - 2} \right)^{-(\nu_m + (1+p)d)/2} \leq 1. \quad (\text{B.17})$$

Hence, $t_d(\mathbf{y}_t; \mu_{m,t}, \Omega_{m,t}, \nu_m + dp) \leq \left(\frac{c_3 - 2}{c_4 + dp - 2} \right)^{-d/2} c_2 c_6$. It then follows from $\sum_{m=1}^M \alpha_{m,t} = 1$ that

$$l_t(\boldsymbol{\theta}) \leq \log \left(\max \left\{ (2\pi)^{-d/2} c_2, \left(\frac{c_3 - 2}{c_4 + dp - 2} \right)^{-d/2} c_2 c_6 \right\} \right) < \infty. \quad (\text{B.18})$$

That is, $l_t(\boldsymbol{\theta})$ is bounded from above by a finite constant.

Next, we proceed by bounding $l_t(\boldsymbol{\theta})$ from below. Since the eigenvalues of Ω_m^{-1} are continuous functions of the parameters bounded by compactness of the parameter space, the largest eigenvalue, λ_2^{max} , is bounded from above by some finite constant, say c_9 . Making use of the orthonormal spectral decomposition of Ω_m^{-1} , we then obtain

$$\begin{aligned} (\mathbf{y}_t - \mu_{m,t})'\Omega_m^{-1}(\mathbf{y}_t - \mu_{m,t}) &\leq \lambda_2^{max} (\mathbf{y}_t - \mathbf{A}_{m,p}\mathbf{y}_{t-1})'(\mathbf{y}_t - \mathbf{A}_{m,p}\mathbf{y}_{t-1}) \\ &\leq c_9 (\mathbf{y}'_t \mathbf{y}_t - 2\mathbf{y}'_t \mathbf{A}_{m,p} \mathbf{y}_{t-1} + \mathbf{y}'_{t-1} \mathbf{A}'_{m,p} \mathbf{A}_{m,p} \mathbf{y}_{t-1}). \end{aligned} \quad (\text{B.19})$$

The compactness of the parameter space implies that

$$\mathbf{y}'_{t-1} \mathbf{A}'_{m,p} \mathbf{A}_{m,p} \mathbf{y}_{t-1} \leq c_{10} \sum_{i=1}^{dp} \sum_{j=1}^{dp} |\mathbf{y}_{j,t-1} \mathbf{y}_{i,t-1}| \quad (\text{B.20})$$

for some finite constant c_{10} , where $\mathbf{y}_{i,t-1}$ is the i th element of \mathbf{y}_{t-1} . Denoting by $a_{m,i}(k, j)$ the kj th element of the autoregression matrix $\mathbf{A}_{m,i}$ and y_{kt} the k th element of \mathbf{y}_t , we have

$$\mathbf{y}'_t \mathbf{A}_{m,p} \mathbf{y}_{t-1} = \sum_{k=1}^d \sum_{i=1}^p \sum_{j=1}^d a_{m,i}(k, j) y_{kt} y_{j,t-1} \leq \sum_{k=1}^d \sum_{i=1}^p \sum_{j=1}^d c_{11} |y_{kt} y_{j,t-1}|, \quad (\text{B.21})$$

where c_{11} is a finite constant that bounds the absolute values of the autoregression coefficients from above (which exists due to compactness of the parameter space). Combining the above two bounds with (B.19) gives the upper bound

$$(\mathbf{y}_t - \mu_{m,t})'\Omega_m^{-1}(\mathbf{y}_t - \mu_{m,t}) \leq c_{12} \left(\mathbf{y}'_t \mathbf{y}_t + \sum_{i=1}^{dp} \sum_{j=1}^{dp} |\mathbf{y}_{j,t-1} \mathbf{y}_{i,t-1}| + \sum_{k=1}^d \sum_{i=1}^p \sum_{j=1}^d |y_{kt} y_{j,t-1}| \right). \quad (\text{B.22})$$

where c_{12} is a finite constant.

Using the fact that $\Sigma_{m,p}^{-1}$ is positive definite together with the bounds $2 < c_3 \leq \nu_m \leq c_4 < \infty$ shows that

$$\Omega_{m,t}^{-1} = \frac{\nu_m - 2 + dp}{\nu_m - 2 + (\mathbf{y}_{t-1} - \mathbf{1}_p \otimes \mu_m)' \Sigma_{m,p}^{-1} (\mathbf{y}_{t-1} - \mathbf{1}_p \otimes \mu_m)} \Omega_m^{-1} \leq \frac{c_4 - 2 + dp}{c_3 - 2} \Omega_m^{-1}. \quad (\text{B.23})$$

Using the above inequality together with $2 < c_3 \leq \nu_m$ and (B.22) then gives

$$\frac{(\mathbf{y}_t - \mu_{m,t})' \Omega_{m,t}^{-1} (\mathbf{y}_t - \mu_{m,t})}{\nu_m + pd - 2} \leq c_{13} \left(y'_t y_t + \sum_{i=1}^{dp} \sum_{j=1}^{dp} |\mathbf{y}_{j,t-1} \mathbf{y}_{i,t-1}| + \sum_{k=1}^d \sum_{i=1}^p \sum_{j=1}^d |y_{kt} y_{jt-i}| \right), \quad (\text{B.24})$$

where $c_{13} = ((c_3 - 2)(c_3 + pd - 2))^{-1} (c_4 - 2 + dp) c_{12}$ is a finite constant.

From $\sum_{m=1}^M \alpha_{m,t} = 1$, (B.10), (B.13), (B.16), (B.22), (B.24), and $\nu_m \leq c_4$, we then obtain a lower bound for $l_t(\boldsymbol{\theta})$ as

$$\begin{aligned} l_t(\boldsymbol{\theta}) \geq & \min \left\{ -\frac{d}{2} \log(2\pi) + \log(c_1) \right. \\ & - \frac{1}{2} c_{12} \left(y'_t y_t + \sum_{i=1}^{dp} \sum_{j=1}^{dp} |\mathbf{y}_{j,t-1} \mathbf{y}_{i,t-1}| + \sum_{k=1}^d \sum_{i=1}^p \sum_{j=1}^d |y_{kt} y_{jt-i}| \right), \\ & c_{15} - \frac{d}{2} \log(c_4 - 2 + c_7 (\mathbf{y}'_{t-1} \mathbf{y}_{t-1} - 2c_8 \mathbf{y}'_{t-1} \mathbf{1}_{dp} + dpc_8^2)) \\ & \left. - c_{14} \log \left(1 + c_{13} \left(y'_t y_t + \sum_{i=1}^{dp} \sum_{j=1}^{dp} |\mathbf{y}_{j,t-1} \mathbf{y}_{i,t-1}| + \sum_{k=1}^d \sum_{i=1}^p \sum_{j=1}^d |y_{kt} y_{jt-i}| \right) \right) \right\}, \quad (\text{B.25}) \end{aligned}$$

where $c_{14} = (c_4 + (1+p)d)/2$ and $c_{15} = \log(c_5) + \log(c_1) + \frac{d}{2}(c_3 - 2 + dp)$. Since y_t is stationary with finite second moments, it holds that

$$\begin{aligned} E \left[y'_t y_t + \sum_{i=1}^{dp} \sum_{j=1}^{dp} |\mathbf{y}_{j,t-1} \mathbf{y}_{i,t-1}| + \sum_{k=1}^d \sum_{i=1}^p \sum_{j=1}^d |y_{kt} y_{jt-i}| \right] &< \infty \quad \text{and} \\ E[\mathbf{y}'_{t-1} \mathbf{y}_{t-1} - 2c_8 \mathbf{y}'_{t-1} \mathbf{1}_{dp}] &< \infty, \quad (\text{B.26}) \end{aligned}$$

and thereby we obtain from Jensen's inequality that also

$$E \left[\log \left(1 + c_{13} \left(y'_t y_t + \sum_{i=1}^{dp} \sum_{j=1}^{dp} |\mathbf{y}_{j,t-1} \mathbf{y}_{i,t-1}| + \sum_{k=1}^d \sum_{i=1}^p \sum_{j=1}^d |y_{kt} y_{jt-i}| \right) \right) \right] < \infty \quad \text{and} \quad (\text{B.27})$$

$$E[\log(c_4 - 2 + c_7 (\mathbf{y}'_{t-1} \mathbf{y}_{t-1} - 2c_8 \mathbf{y}'_{t-1} \mathbf{1}_{dp} + dpc_8^2))] < \infty.$$

The upper bound (B.18) together with (B.25), (B.26), and (B.27) shows that $E[\sup_{\boldsymbol{\theta} \in \Theta} |l_t(\boldsymbol{\theta})|] < \infty$. ■

Proof of (ii). To prove that $E[l_t(\boldsymbol{\theta})]$ is uniquely maximized at $\boldsymbol{\theta} = \boldsymbol{\theta}_0$, it needs to be shown that $E[l_t(\boldsymbol{\theta})] \leq E[l_t(\boldsymbol{\theta}_0)]$, and that $E[l_t(\boldsymbol{\theta})] = E[l_t(\boldsymbol{\theta}_0)]$ implies

$$\begin{aligned} \boldsymbol{\vartheta}_m &= \boldsymbol{\vartheta}_{\tau(m),0} \quad \text{and} \quad \alpha_m = \alpha_{\tau(m),0} \quad \text{when} \quad m = 1, \dots, M_1, \quad \text{and} \\ (\boldsymbol{\vartheta}_m, \nu_m) &= (\boldsymbol{\vartheta}_{\tau(m),0}, \nu_{\tau(m),0}) \quad \text{and} \quad \alpha_m = \alpha_{\tau(m),0} \quad \text{when} \quad m = M_1 + 1, \dots, M, \quad (\text{B.28}) \end{aligned}$$

for some permutations $\{\tau_1(1), \dots, \tau_1(M_1)\}$ and $\{\tau_2(M_1 + 1), \dots, \tau_2(M)\}$. For notational clarity, we write $\mu_{m,t} = \mu(\mathbf{y}; \boldsymbol{\vartheta}_m)$, $\Omega_m = \Omega(\boldsymbol{\vartheta}_m)$, $\Omega_{m,t} = \Omega(\mathbf{y}; \boldsymbol{\vartheta}_m, \nu_m)$, and $\alpha_{m,t} = \alpha_m(\mathbf{y}; \boldsymbol{\theta})$, making clear their dependence on the parameter value.

The density of (y_t, \mathbf{y}_{t-1}) can be written as

$$f((y_t, \mathbf{y}_{t-1}); \boldsymbol{\theta}_0) = \sum_{n=1}^M \alpha_{n,0} d_{n,dp}(\mathbf{y}_{t-1}; \mathbf{1}_p \otimes \mu_{n,0}, \Sigma_{n,p,0}, \nu_{n,0}) \times \left(\sum_{m=1}^{M_1} \alpha_m(\mathbf{y}; \boldsymbol{\theta}_0) n_d(y_t; \mu(\mathbf{y}; \boldsymbol{\vartheta}_{m,0}), \Omega(\boldsymbol{\vartheta}_{m,0})) + \sum_{m=M_1+1}^M \alpha_m(\mathbf{y}; \boldsymbol{\theta}_0) t_d(y_t; \mu(\mathbf{y}; \boldsymbol{\vartheta}_{m,0}), \Omega(\mathbf{y}; \boldsymbol{\vartheta}_{m,0}, \nu_{m,0}), \nu_{m,0} + dp) \right), \quad (\text{B.29})$$

where $d_{n,dp}(\cdot; \mathbf{1}_p \otimes \mu_{n,0}, \Sigma_{n,p,0}, \nu_{n,0})$ is defined in (3.4). By using this together with reasoning based on Kullback-Leibler divergence, arguments analogous to those in Kalliovirta *et al.* (2016, pp. 494-495) can be used to conclude that $E[l_t(\boldsymbol{\theta})] - E[l_t(\boldsymbol{\theta}_0)] \leq 0$, with equality if and only if for almost all $(y, \mathbf{y}) \in \mathbb{R}^{d(p+1)}$,

$$\begin{aligned} & \sum_{m=1}^{M_1} \alpha_m(\mathbf{y}; \boldsymbol{\theta}) n_d(y_t; \mu(\mathbf{y}; \boldsymbol{\vartheta}_m), \Omega(\boldsymbol{\vartheta}_m)) + \\ & \sum_{m=M_1+1}^M \alpha_m(\mathbf{y}; \boldsymbol{\theta}) t_d(y_t; \mu(\mathbf{y}; \boldsymbol{\vartheta}_m), \Omega(\mathbf{y}; \boldsymbol{\vartheta}_m, \nu_m), \nu_m + dp) \\ & = \sum_{m=1}^{M_1} \alpha_m(\mathbf{y}; \boldsymbol{\theta}_0) n_d(y_t; \mu(\mathbf{y}; \boldsymbol{\vartheta}_{m,0}), \Omega(\boldsymbol{\vartheta}_{m,0})) + \\ & \sum_{m=M_1+1}^M \alpha_m(\mathbf{y}; \boldsymbol{\theta}_0) t_d(y_t; \mu(\mathbf{y}; \boldsymbol{\vartheta}_{m,0}), \Omega(\mathbf{y}; \boldsymbol{\vartheta}_{m,0}, \nu_{m,0}), \nu_{m,0} + dp). \end{aligned} \quad (\text{B.30})$$

For each fixed \mathbf{y} at a time, the mixing weights, conditional means, and conditional covariances in (B.30) are constants, so we may apply the result on identification of finite mixtures of multivariate Gaussian and t -distributions in Holzmann, Munk, and Gneiting (2006, Example 1) (their parametrization of the t -distribution slightly differs from ours, but identification with their parametrization implies identification with our parametrization). For each fixed \mathbf{y} , there thus exists a permutations $\{\tau_1(1), \dots, \tau_1(M_1)\}$ and $\{\tau_2(M_1 + 1), \dots, \tau_2(M)\}$ (that may depend on \mathbf{y}) of the index sets $\{1, \dots, M_1\}$ and $\{M_1 + 1, \dots, M\}$ such that

$$\alpha_m(\mathbf{y}; \boldsymbol{\theta}) = \alpha_{\tau_1(m)}(\mathbf{y}; \boldsymbol{\theta}_0), \quad \mu(\mathbf{y}; \boldsymbol{\vartheta}_m) = \mu(\mathbf{y}; \boldsymbol{\vartheta}_{\tau_1(m),0}), \quad \text{and} \quad \Omega(\boldsymbol{\vartheta}_m) = \Omega(\boldsymbol{\vartheta}_{\tau_1(m),0}), \quad (\text{B.31})$$

for $m = 1, \dots, M_1$ and almost all $y \in \mathbb{R}^d$, and

$$\begin{aligned} & \alpha_m(\mathbf{y}; \boldsymbol{\theta}) = \alpha_{\tau_2(m)}(\mathbf{y}; \boldsymbol{\theta}_0), \quad \mu(\mathbf{y}; \boldsymbol{\vartheta}_m) = \mu(\mathbf{y}; \boldsymbol{\vartheta}_{\tau_2(m),0}), \quad \Omega(\mathbf{y}; \boldsymbol{\vartheta}_m) = \Omega(\mathbf{y}; \boldsymbol{\vartheta}_{\tau_2(m),0}), \\ & \text{and} \quad \nu_m = \nu_{\tau_2(m),0} \end{aligned} \quad (\text{B.32})$$

for $m = M_1 + 1, \dots, M$ and almost all $\mathbf{y} \in \mathbb{R}^d$. Note that from (B.31) we readily obtain $\text{vech}(\Omega_m) = \text{vech}(\Omega_{\tau_1(m),0})$.

Arguments analogous to those in Kalliovirta *et al.* (2016, p. 495) can then be used to conclude from (B.31) and (B.32) that $\alpha_m = \alpha_{\tau_1(m),0}$, $\phi_{m,0} = \phi_{\tau_1(m),0,0}$, and $\mathbf{A}_{m,p} = \mathbf{A}_{\tau_1(m),p,0}$ for $m = 1, \dots, M_1$, and $\alpha_m = \alpha_{\tau_2(m),0}$, $\phi_{m,0} = \phi_{\tau_2(m),0,0}$, and $\mathbf{A}_{m,p} = \mathbf{A}_{\tau_2(m),p,0}$ for $m = M_1 + 1, \dots, M$. Given these identities and $\nu_m = \nu_{\tau_2(m),0}$, we obtain from $\Omega(\mathbf{y}; \boldsymbol{\vartheta}_m) = \Omega(\mathbf{y}; \boldsymbol{\vartheta}_{\tau_2(m),0})$ in (B.32) that

$$\begin{aligned} & (\mathbf{y} - \mathbf{1}_p \otimes \mu_{\tau_2(m),0})' \Sigma_p(\boldsymbol{\vartheta}_m)^{-1} (\mathbf{y} - \mathbf{1}_p \otimes \mu_{\tau_2(m),0}) \Omega_m - \\ & (\mathbf{y} - \mathbf{1}_p \otimes \mu_{\tau_2(m),0})' \Sigma_p(\boldsymbol{\vartheta}_{\tau_2(m),0})^{-1} (\mathbf{y} - \mathbf{1}_p \otimes \mu_{\tau_2(m),0}) \Omega_{\tau_2(m),0} = (\nu_{\tau_2(m),0} - 2)(\Omega_{\tau_2(m),0} - \Omega_m). \end{aligned} \quad (\text{B.33})$$

The condition $\Omega(\mathbf{y}; \boldsymbol{\vartheta}_m) = \Omega(\mathbf{y}; \boldsymbol{\vartheta}_{\tau_2(m),0})$ implies that Ω_m is proportional to $\Omega_{\tau_2(m),0}$, say $\Omega_m = c(\boldsymbol{\vartheta}_{m,\tau_2(m)}^+) \Omega_{\tau_2(m),0}$, where the strictly positive scalar $c(\boldsymbol{\vartheta}_{m,\tau_2(m)}^+)$ may depend on the parameter $\boldsymbol{\vartheta}_{m,\tau_2(m)}^+ \equiv (\boldsymbol{\vartheta}_m, \boldsymbol{\vartheta}_{\tau_2(m),0}, \nu_{\tau_2(m),0})$. It is then easy to see from the vectorized structure of $\Sigma_p(\cdot)$, given in (2.4), that $\Sigma_p(\boldsymbol{\vartheta}_m)^{-1} = c(\boldsymbol{\vartheta}_{m,\tau_2(m)}^+)^{-1} \Sigma_p(\boldsymbol{\vartheta}_{\tau_2(m),0})^{-1}$. By using this together with the identity $\Omega_m = c(\boldsymbol{\vartheta}_{m,\tau_2(m)}^+) \Omega_{\tau_2(m),0}$, the left hand side of (B.33) reduces to

$$\begin{aligned} & (\mathbf{y} - \mathbf{1}_p \otimes \mu_{\tau_2(m),0})' (c(\boldsymbol{\vartheta}_{m,\tau_2(m)}^+) \Sigma_p(\boldsymbol{\vartheta}_m)^{-1} - \Sigma_p(\boldsymbol{\vartheta}_{\tau_2(m),0})^{-1}) (\mathbf{y} - \mathbf{1}_p \otimes \mu_{\tau_2(m),0}) \Omega_{\tau_2(m),0} \\ & = (\mathbf{y} - \mathbf{1}_p \otimes \mu_{\tau_2(m),0})' \left(\frac{c(\boldsymbol{\vartheta}_{m,\tau_2(m)}^+)}{c(\boldsymbol{\vartheta}_{m,\tau_2(m)}^+)} \Sigma_p(\boldsymbol{\vartheta}_{\tau_2(m),0})^{-1} - \Sigma_p(\boldsymbol{\vartheta}_{\tau_2(m),0})^{-1} \right) (\mathbf{y} - \mathbf{1}_p \otimes \mu_{\tau_2(m),0}) \\ & \times \Omega_{\tau_2(m),0} = 0. \end{aligned} \quad (\text{B.34})$$

Thereby (B.33) reduces to $(\nu_{\tau_2(m),0} - 2)(\Omega_{\tau_2(m),0} - \Omega_m) = 0$, which implies $\Omega_m = \Omega_{\tau_2(m),0}$, as $\nu_{\tau_2(m),0} > 2$. Since the condition (5.3) sets a unique ordering for the mixture components, it follows that $\boldsymbol{\theta} = \boldsymbol{\theta}_0$, completing the proof of consistency.

Given consistency and assumptions of the theorem, asymptotic normality of the ML estimator can be concluded using the standard arguments. The required steps can be found, for example, in Kalliovirta *et al.* (2016, proof of Theorem 3). We omit the details for brevity. ■

Appendix C Details on the empirical application

C.1 Model selection and adequacy of the selected model

We estimated the models based on the exact log-likelihood function.¹⁴ The estimation and other numerical analysis is carried out with the CRAN distributed R package `gmvarKit` Virolainen (2018a)

¹⁴We disregarded estimates that incorporated a near-singular error term covariance matrix or only a few observations from one of the regimes, and considered the largest local maximum of the log-likelihood function that incorporates clearly non-singular error term covariance matrices and a reasonable amount of observations from both regimes. While our procedure is open for discussion, note that the disregarded estimates are useless for statistical inference, as the number of observations from the more rare regime is very small compared to the number of parameters. Such

that accompanies this paper. The R package `gmvarKit` also contains the data studied in the empirical application to conveniently allow the reproduction of our results. For evaluating adequacy of the estimated models, we employ quantile residuals diagnostics in the framework proposed by Kalliovirta and Saikkonen (2010). For a correctly specified G-StMVAR model, the multivariate quantile residuals are asymptotically standard normally distributed and can thereby be used for graphical diagnostics similarly to the conventional Pearson residuals (Kalliovirta and Saikkonen, 2010, Lemma 3).¹⁵ For brevity, we show the diagnostic figures for the selected model only.

We started by estimating one-regime StMVAR models with autoregressive orders $p = 1, \dots, 12$ and found that BIC, HQIC, and AIC were all minimized by the order $p = 1$. Graphical quantile residual diagnostics revealed that the StMVAR(1, 1) model is somewhat inadequate particularly in capturing conditional heteroskedasticity of the series and movements of the interest rate variable, whose quantile residuals' time series displays a shift in volatility and marginal distribution significant excess kurtosis. Increasing the autoregressive order to 2 or 3 did not help much. Moreover, increasing p from 2 to 3 decreased the log-likelihood, suggesting that the order $p = 3$ might not be suitable for a StMVAR model. The log-likelihoods and values of the information criteria are presented in Table 1 for the discussed models.

As the one-regime models were found inadequate, we estimated a two-regime StMVAR model with $p = 1$, i.e., a G-StMVAR($p = 1, M_1 = 0, M_2 = 2$) model. Compared to the one-regime models, particularly the time series plot and marginal distribution of the interest variable's quantile residuals became significantly more reasonable. However, we found that this model has several moderately sized correlation coefficients (CC) at small lags in the autocorrelation function (ACF) of its quantile residuals and squared quantile residuals. To improve the fitness, we increased the autoregressive order to $p = 2$, which decreased many of the moderately sized CCs but increased AIC (see Table 1). The AIC is, nevertheless, smaller than for any of the one-regime models (while the one-regime StMVAR $p = 1, 2$ models have smaller BIC and the $p = 1$ model also smaller HQIC). As is discussed next, we find the overall adequacy of this model reasonable.¹⁶

estimates arise due to the complex endogeneity of the mixing weights that makes the surface of the log-likelihood function extremely complex. Similar puzzle in the estimation is discussed in univariate context in more detail in the vignette of the R package `uGMAR` (Virolainen, 2018b).

¹⁵Kalliovirta and Saikkonen (2010) also propose formal diagnostic tests for testing normality, autocorrelation, and conditional heteroskedasticity of the quantile residuals. The tests take into account the uncertainty about the true parameter value and can be calculated based on the observed data or by employing a simulation procedure for better size properties. However, we found these tests quite forgiving without the simulation procedure, while with the simulation procedure using a sample of length 10000, all the tests rejected the adequacy our StMVAR model at all the conventional levels of significance. We therefore rather employ graphical diagnostics to examine to what extent the statistical properties of the quantile residuals plausibly resemble those on an IID standard normal process.

¹⁶It is possible that superior fitness of the two-regime models is due to the accommodation of regime-switching error covariance matrices or kurtosis and cannot be attributed to the time-varying AR matrices or intercepts. To test whether this is the case, we estimated two constrained StMVAR(2, 2) models. In the first one, we constrained the AR matrices to identical in both regimes, whereas in the second one, we constrained AR matrices and intercepts to be identical in both regimes. Because these models are nested to the unconstrained StMVAR model, the constraints can be tested with a likelihood ratio test (assuming the validity of the unverified assumptions made in Theorem 3). The former type constraints obtained the p -value 0.022 and the latter type constraints the p -value $2 \cdot 10^{-4}$. We then repeated the exercise for the StMVAR(1, 2) model, which minimized AIC, and obtained the p -values 0.003 and $2 \cdot 10^{-7}$ for constraints, respectively. As the constraints are rejected at the 5% level of significance or less, it seems plausible that AR matrices and intercepts vary in time.

| Model | Log-lik | BIC | HQIC | AIC |
|--------------|---------|-------|-------|-------|
| StMVAR(1, 1) | -2.486 | 5.604 | 5.360 | 5.197 |
| StMVAR(2, 1) | -2.447 | 5.851 | 5.482 | 5.235 |
| StMVAR(3, 1) | -2.471 | 6.224 | 5.729 | 5.398 |
| StMVAR(1, 2) | -2.211 | 5.705 | 5.210 | 4.878 |
| StMVAR(2, 2) | -2.138 | 6.210 | 5.464 | 4.964 |

Table 1: The log-likelihoods and values of the information criteria divided by the number of observations for the discussed StMVAR(p, M) models.

Figure 3 presents the ACF and crosscorrelation function (CCF) of the quantile residuals of the StMVAR(2, 2) model for the first 20 lags. As the figure shows, there is not much autocorrelation in the residuals, but CCs of almost 0.2 in absolute value stick out in the ACF of IPI’s quantile residuals at the lag 10, in the CCF of OIL and HCPI at the lag 6, and in the CCF of HCPI and RATE at the lag 15. There are also a moderately sized CCs at small lags in the ACF of the IPI’s quantile residuals at the lag 3 and in the RATE’s quantile residuals at the lag 2. These CCs are not, however, very large, and as 316 CCs are presented, some of them are expected to be moderate for a correctly specified model. Therefore, our model appears to capture the autocorrelation structure of the series reasonably well, although some of the CCs are slightly larger than what one would expect for an IID process.¹⁷

The ACF and CCF of the squared quantile residuals are presented in Figure 4 for the first 20 lags. The figure shows that there is a moderately large CC at the first lag in the ACF of the IPI’s squared quantile residuals and a slightly larger one (roughly 0.2) at the fourth lag in the ACF of RATE’s squared quantile residuals. There is a particularly large CC at the lag 10 in the CCF of HCPI’s and IPI’s squared quantile residuals, and a somewhat large CC at the lag 16 in the CCF of IPI’s and RATE’s squared quantile residuals, at the lag 9 in the CCF of OIL’s and IPI’s squared quantile residuals, and at the lag 10 in the OIL’s and HCPI’s squared quantile residuals. Nonetheless, the model seems to capture the conditional heteroskedasticity of the series moderately well, as the inadequacies do not seem very severe, with the exception of the single large CC at the lag 10 in the CCF between squared quantile residuals of HCPI and IPI.

¹⁷It does not show up in the figure but there is a large negative CC at the lag 24 in autocorrelation function the IPI’s quantile residuals. We suspect that this might be related to the employed detrending method (Hamilton, 2018), where the cyclical component of IPI_t at the time $t+h$ is defined as the OLS residual from regressing IPI_{t+h} on a constant and $IPI_t, \dots, IPI_{t-s+1}$, where we used $h = 24$ and $s = 12$. So we experimented with the univariate log industrial production series and detrended it with the filter using $h = 5, 6, 7, 10, 12, 18, 19, 24$ and $s = 12$. First, we examined the partial autocorrelation functions (PACF) of the cyclical component and found that with each h , there is a large or moderate positive partial autocorrelation coefficient (PACC) at the lags $h + 1$ and $2h + 1$ with the latter one being smaller. Except that for $h = 24$ both of the PACCs were quite small, however, and for $h = 19$ the PACC at the lag $2h + 1$ was relatively small. Then, we fitted one-regime GMAR and StMAR models (Kalliovirta *et al.*, 2015, Meitz *et al.*, forthcoming) to the cyclical component using the autoregressive orders $p = 2, 3, 11, 12$ and examined the autocorrelation functions of the quantile residuals (which equal to the Pearson residuals in the linear Gaussian case, see Kalliovirta, 2012, for details). In each of the cases, there was a large negative CC in the quantile residuals’ ACF at the lag h when $p \leq h$ but not when $p > h$ (in which case there was often a large negative CC at some lag larger than p). Hence, the large negative CC seems to be related the detrending method. Nonetheless, since accommodating the large negative CC with the autoregressive order $p = 25$ seems excessive even for a linear VAR (given our sample of 276 observations), we will only note its existence. The details of this investigation are not shown for brevity.

The marginal quantile residual time series are presented in the top panels of Figure 5. The time series seem reasonable, as there are no apparent shifts in the mean, volatility, or dynamics. The COVID-19 lockdown shows as a large negative (marginal) quantile residual of IPI, but we do not view this as an inadequacy, as the fast drop in the cycle is known to be caused by an exceptionally large exogenous shock, and a correctly specified model should thereby produce a large negative residual. Also, the relatively high inflation rates during the COVID-19 crisis show as consecutive positive (marginal) quantile residuals of HCPI. The normal quantile-quantile plots (the bottom panels of Figure 5) show that the marginal distribution of the series appears to be captured relatively well. Overall, we find the adequacy of our model reasonable enough for further analysis.

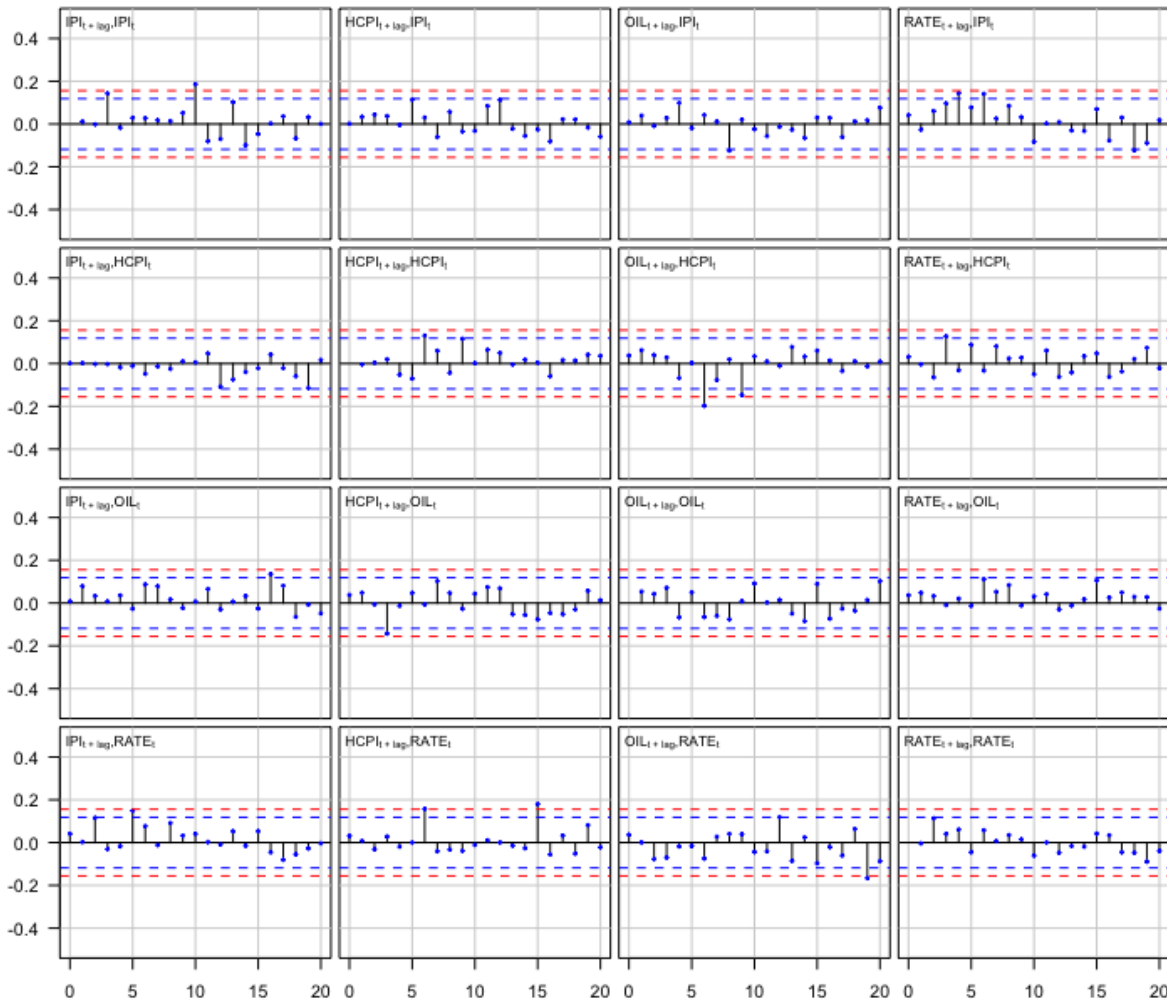


Figure 3: Auto- and crosscorrelation functions of the quantile residuals of the fitted StMVAR(2, 2) model for the lags 0, 1, ..., 20. The lag zero autocorrelation coefficients are omitted, as they are one by convention. The blue dashed lines are the 95% bounds $\pm 1.96/\sqrt{T}$ ($T = 274$ as the first $p = 2$ observations were used as the initial values) for autocorrelations of IID observations, whereas the red dashed lines are the corresponding 99% bounds $\pm 2.58/\sqrt{T}$. These bounds are presented to give an approximate perception on the magnitude of the correlation coefficients.

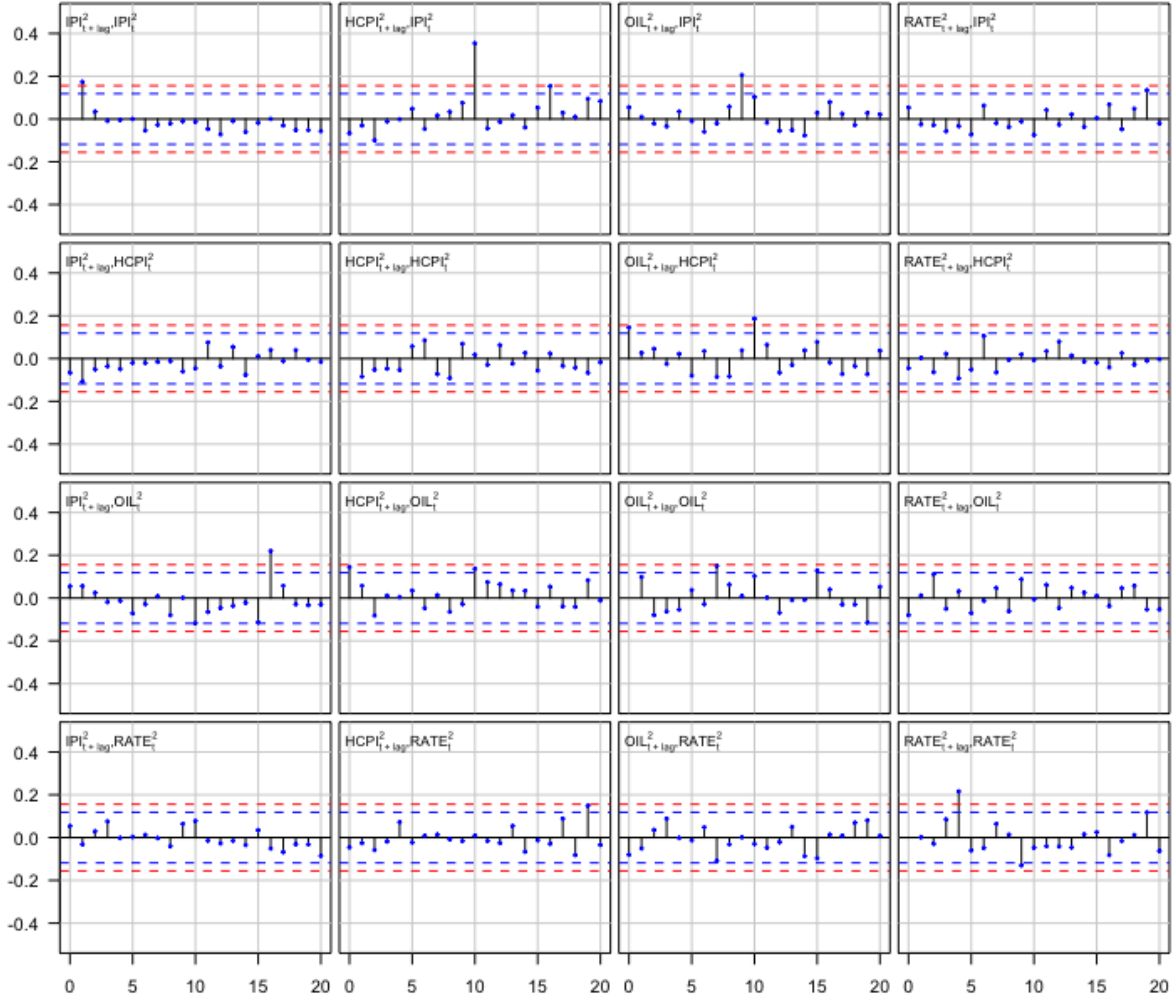


Figure 4: Auto- and crosscorrelation functions of the squared quantile residuals of the fitted StMVAR(2, 2) model for the lags 0, 1, ..., 20. The lag zero autocorrelation coefficients are omitted, as they are one by convention. The blue dashed lines are the 95% bounds $\pm 1.96/\sqrt{T}$ ($T = 274$ as the first $p = 2$ observations were used as the initial values) for autocorrelations of IID observations, whereas the red dashed lines are the corresponding 99% bounds $\pm 2.58/\sqrt{T}$. These bounds are presented to give an approximate perception on the magnitude of the correlation coefficients.

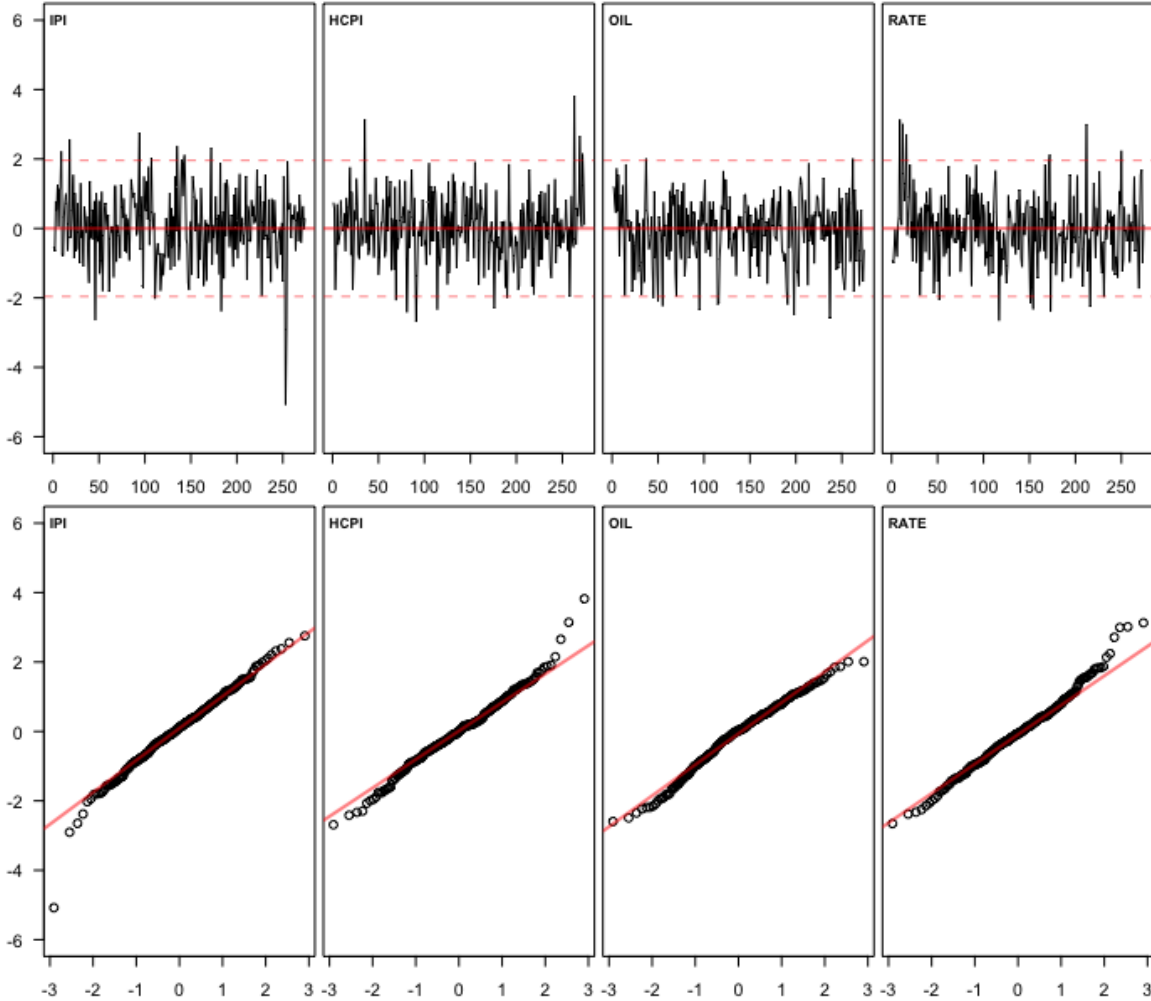


Figure 5: Quantile residual time series and normal quantile-quantile-plots of the fitted StMVAR(2, 2) model.

C.2 Characteristics of the selected model

Table 2 presents the estimates for the mixing weight parameters, degrees of freedom parameters, and the estimated unconditional means and variances of each marginal series (based on the stationary properties of our model). The mixing weight parameters have the interpretation of being the unconditional probabilities for an observation being generated from each regime. For a correctly specified model, they should hence approximately reflect the proportions of observations generated from each regime. The first regime has a mixing weight parameter estimate 0.77, and it covers approximately 63% of the series (approximated as the mean of the estimated mixing weights), whereas the second regime has the implied mixing weight parameter estimate 0.23 and it covers approximately 37% of the series. Therefore, they are somewhat disproportionate, but seem reasonable enough not to distort the generalized impulse response functions too much.

The degrees of freedom parameter estimates in Table 2 show that the first regime has fatter tailed

| | | | <i>IPI</i> | | <i>HCPI</i> | | <i>OIL</i> | | <i>RATE</i> | |
|----------|------------------|---------------|-------------------|------------------------|-------------------|------------------------|-------------------|------------------------|-------------------|------------------------|
| | $\hat{\alpha}_m$ | $\hat{\nu}_m$ | $\hat{\mu}_{m,1}$ | $\hat{\sigma}_{m,1}^2$ | $\hat{\mu}_{m,2}$ | $\hat{\sigma}_{m,2}^2$ | $\hat{\mu}_{m,3}$ | $\hat{\sigma}_{m,3}^2$ | $\hat{\mu}_{m,4}$ | $\hat{\sigma}_{m,4}^2$ |
| Regime 1 | 0.77 | 3.40 | -2.89 | 111.22 | 0.12 | 0.08 | 0.02 | 1.79 | 0.24 | 78.96 |
| Regime 2 | 0.23 | 12.89 | 2.79 | 10.25 | 0.19 | 0.02 | 0.33 | 0.77 | 2.71 | 0.47 |

Table 2: Mixing weight parameter estimates ($\hat{\alpha}_m$), degrees of freedom parameter estimates ($\hat{\nu}_m$), and marginal stationary means ($\hat{\mu}_{m,i}$) and variances ($\hat{\sigma}_{m,i}^2$) of the component series implied by the fitted StMVAR(2, 2) model for each of the regimes.

distribution than the second one. The first regime also has negative and volatile long-run output gap, while the second regime has positive and less volatile long-run output gap. Long-run inflation, is low in the first regime (roughly 1.4% yearly), whereas it is moderate in the second regime (roughly 2.3% yearly). Also oil price inflation is relatively low in first regime, whereas it is high in the second one.¹⁸ The interest rate variable has low mean in first regime, but the variance is high, which reflects wandering movements of the shadow rate (Wu and Xia, 2016) after the early 2010's recession. In the second regime, the interest rate variable has moderate mean and low variance. According to the unconditional variances of the observable variables in Table 2, the first regime appears overall more volatile than the second.

According to the estimated mixing weights presented in Figure 1, the first regime (blue) mainly prevails after the collapse of Lehman Brothers in the Financial crisis in September 2008. The first regime also obtains large mixing weights during and before the early 2000's recession, however. The second regime (red) dominates when the first one does not; that is, mainly before the Financial crisis, but excluding the aforementioned periods when the first regime obtains large mixing weights. After the Financial crisis, the second regime's mixing weights stay close to zero, excluding a short period before the early 2010's recession. Because the first regime is characterized by negative output gap and it mainly prevails after the Financial crisis, we refer to it as the low-growth post-Financial crisis regime. Accordingly, because the second regime is characterized by positive output gap and it mainly prevails before the Financial crisis, we refer to it as the high-growth pre-Financial crisis regime.

C.3 Estimates of the structural parameters

The constraints imposed on the B-matrix of the StMVAR(2, 2) model in Section 7.1 produced the following estimates:

$$\hat{W} = \begin{bmatrix} 0.88 (0.692) & -1.16 (0.812) & 2.00 (1.164) & -0.40 (0.351) \\ -0.13 (0.091) & 0.14 (0.099) & 0.20 (0.122) & 0 \\ -1.20 (0.686) & -0.42 (0.561) & 0.65 (0.435) & 0 \\ 0.01 (0.021) & -0.03 (0.029) & 0.06 (0.045) & 0.56 (0.313) \end{bmatrix}, \quad \hat{\lambda}_2 = \begin{bmatrix} 0.37 (0.423) \\ 0.27 (0.303) \\ 0.14 (0.161) \\ 0.02 (0.027) \end{bmatrix}, \quad (\text{C.1})$$

¹⁸The log-difference of oil price was multiplied by 10 and not 100 for numerical reasons, so the unconditional means should be multiplied 10 to obtain estimates for the (approximate) monthly long-run oil price inflation in percentage units.

where the identified monetary policy shock is ordered last. The approximate standard errors are presented in parentheses next to the estimates.